



Swansea University
Prifysgol Abertawe



Cronfa - Swansea University Open Access Repository

This is an author produced version of a paper published in:

AIAA Journal

Cronfa URL for this paper:

<http://cronfa.swan.ac.uk/Record/cronfa36669>

Paper:

Scarth, C. & Adhikari, S. (2017). Modeling Spatially Varying Uncertainty in Composite Structures Using Lamination Parameters. *AIAA Journal*, 55(11), 3951-3965.

<http://dx.doi.org/10.2514/1.J055705>

This item is brought to you by Swansea University. Any person downloading material is agreeing to abide by the terms of the repository licence. Copies of full text items may be used or reproduced in any format or medium, without prior permission for personal research or study, educational or non-commercial purposes only. The copyright for any work remains with the original author unless otherwise specified. The full-text must not be sold in any format or medium without the formal permission of the copyright holder.

Permission for multiple reproductions should be obtained from the original author.

Authors are personally responsible for adhering to copyright and publisher restrictions when uploading content to the repository.

<http://www.swansea.ac.uk/library/researchsupport/ris-support/>

Modelling Spatially Varying Uncertainty in Composite Structures using Lamination Parameters

C. Scarth* and S. Adhikari†

College of Engineering, Swansea University, Swansea, United Kingdom

An approach is presented for modelling spatially varying uncertainty in the ply orientations of composite structures. Lamination parameters are used with the aim of reducing the required number of random variables. Karhunen-Loève Expansion (KLE) is employed to decompose the uncertainty in each ply into a sum of random variables and spatially dependent functions. An intrusive Polynomial Chaos Expansion is proposed to approximate the lamination parameters while preserving the separation of the random and spatial dependency. Closed-form expressions are derived for the expansion coefficients in two case studies; an initial example in which uncertainty is modelled using random variables, and a second random field example. The approach is compared against Monte Carlo Simulation results for a variety of layups, as well as closed-form expressions for the mean and covariance. By summing the polynomial chaos basis functions through the laminate thickness, the separation of the random and spatial dependency may be preserved at a laminate level, and the number of random variables reduced for some minimum number of plies. The number of variables increases nonlinearly with the number of KLE terms, and as such, the approach is only beneficial in low order expansions using relatively few KLE terms.

Nomenclature

A	=	in-plane laminate stiffness matrix
\hat{a}_j	=	coefficient of Polynomial Chaos Expansion
a, b, c	=	constants used in ‘generic’ statistical expressions
C	=	covariance function
c	=	correlation length of random field
B	=	extension-bending coupling matrix
D	=	out-of-plane laminate stiffness matrix
\mathcal{D}	=	spatial domain

*NRN Research Fellow, Corresponding author.

†Chair of Aerospace Engineering, AIAA Associate Fellow.

Copyright © 2016 by the American Institute of Aeronautics and Astronautics, Inc. The U.S. Government has a royalty-free license to exercise all rights under the copyright claimed herein for Governmental purposes. All other rights are reserved by the copyright owner.

E	=	expectation operator
E_{11}, E_{22}	=	longitudinal and transverse Young's moduli
f, g	=	functions used in 'generic' statistical expressions
G_{12}	=	shear modulus
H	=	random field
H_p	=	univariate Hermite polynomial of order p
h	=	laminate thickness
L	=	length of spatial domain
\mathbf{M}	=	moment resultants
m	=	number of Karhunen-Loève Expansion terms
\mathbf{N}	=	stress resultants
n	=	number of plies
P	=	number of Polynomial Chaos Expansion terms
p	=	total polynomial order
Q_{ij}	=	reduced lamina stiffnesses
U_i	=	material invariants
X	=	response stochastic process
u_i	=	normalised through-thickness coordinate of the upper surface of i^{th} ply
\mathbf{x}	=	vector of spatial coordinates
\mathbf{y}	=	general vector-valued model output
z_i	=	distance from laminate mid-plane to upper surface of i^{th} ply
α_j	=	multi-index with dictates the order of each univariate orthogonal polynomial
Γ_p	=	Polynomial Chaos Expansion of order p
ϵ^0	=	laminate mid-plane strains
ζ_j	=	standard Gaussian random variable
η_j	=	spatially dependent Karhunen-Loève Expansion terms
θ_i	=	i^{th} ply orientation
κ	=	laminate curvatures
λ_j	=	Karhunen-Loève Expansion eigenvalue
ν_{12}	=	Poisson's ratio

$\xi_{1-4}^{A,B,D}$	=	lamination parameters
σ	=	ply orientation standard deviation
Υ_i	=	random variable used to represent uncertainty at a laminate level
ϕ	=	standard Gaussian Probability Density Function
φ_j	=	Karhunen-Loève Expansion eigenfunction
Ψ_j	=	j^{th} orthogonal polynomial
ω	=	random event from space of possible outcomes

I. Introduction

COMPOSITE materials are being used to an increasing degree, due to a number of benefits including high specific strength and stiffness, and anisotropy which may be exploited to tailor structural properties. While mathematical models can predict behaviour to a high degree of accuracy, in practice all materials and processes are subject to uncertainty. Composite materials require complicated manufacturing processes involving many constituent components, and as such uncertainty can be introduced from a number of sources, such as the the volume fractions and moduli of the fibres,¹ fibre misalignment,² and due to joining and machining techniques.³ Traditionally, uncertainty is accounted for using safety factors and worst-case design scenarios, however, such approaches can be overly conservative, and can inhibit the adoption of new technologies and techniques.⁴

The most commonly used uncertainty quantification technique is Monte Carlo Simulation (MCS), however, this approach can be computationally expensive as a large number of model runs are required to achieve accurate results.⁵ It is therefore also common to use more efficient techniques such as Polynomial Chaos Expansion (PCE),^{6,7} however, the computational effort required by such techniques is known to increase significantly with the number of random variables. The analysis is further complicated when the uncertainty is modelled as random fields, due to the need to discretise these fields. Random fields may be represented using random variables based upon their value at specific spatial coordinates such as finite element midpoints, or using spatial averaging across each element, however, such approaches are mesh dependent.⁸ In spectral techniques such as the Karhunen-Loève Expansion (KLE),⁶ the space of possible outcomes under uncertainty is discretised, resulting in a sum of random variables and spatially dependent functions. In each of the described approaches, modelling random fields can result in a considerable increase in dimensionality compared with the corresponding random variable problem.

Composite material properties have been modelled extensively using random variables. For example, Monte Carlo Simulation was used in,⁹ to model uncertainty in the aeroelastic response of a composite helicopter rotor blade with uncertainty in the elastic moduli. A second-order perturbation technique was used in,¹⁰ to model buckling and

supersonic flutter of laminated plates with uncertainty in the ply orientations, modulus and density, as well as loading and geometric parameters. A similar analysis was undertaken by Oh and Librescu¹¹ for the free vibration of cantilever composite beams. Manan and Cooper¹² used Polynomial Chaos Expansion to model flutter of a cantilever plate wing with uncertainty in the moduli, ply orientations, and thickness. A non-intrusive Polynomial Chaos Expansion was used by Umesh and Ganguli¹³ to model the vibration of smart laminated plates controlled using piezoelectric patches, with uncertainty in the elastic moduli as well as two piezoelectric coefficients. More recently various surrogate models, such as Kriging,¹⁴ RS-HDMR,¹⁵ Gram-Schmidt polynomial chaos expansion¹⁶ and Artificial Neural Network (ANN),¹⁷ have been used in the context of dynamic analysis of composite laminated plates with random parameters.

The application of random field methods to composite material properties was first undertaken by Engelstad and Reddy,¹⁸ who modelled spatially-varying uncertainty in the ply orientations, thickness, and moduli. Random fields were discretised using a Finite Element mesh, and the First Order Second Moment method used to model deflection of a spherical shell, and postbuckling of a flat plate. In,¹⁹ Karhunen-Loève Expansion was combined with a Rayleigh Ritz approach to model free vibration of cantilever plates. Taylor series expansions in the elastic moduli, Poisson's ratio and density were used to express the stiffness and mass matrices as a linear sum of contributions of from each KLE term, thereby enabling the spatial dependency to be integrated directly into these matrices. The Spectral Stochastic Finite Element Method was used in,²⁰ in which KLE is used to represent random fields, Polynomial Chaos Expansion used to model nodal displacements, and an intrusive formulation obtained for the stiffness and mass matrices. Murugan et al.²¹ used a similar approach, in which KLE was used to expand laminate stiffness terms based upon uncertain elastic moduli, and High Dimensional Model Representations were used to determine vibration frequency in the aeroelastic analysis of a composite rotor blade. More recently, KLE was used in conjunction with a non-intrusive polynomial chaos formulation to model free vibration of composite laminates with spatially varying uncertainty in the ply orientations.²² A Stochastic Finite Element approach based upon Optimal Linear Expansion was proposed in²³ for modelling non-Gaussian distributed uncertainty in the elastic moduli and strength of composite laminates. An alternative approach for modelling non-Gaussian fields was proposed²⁴ in which Polynomial Chaos Expansion was combined with a series of nonlinear transformations aimed at matching input marginal distributions at a discrete set of points, and used in the failure analysis of composite laminates.

Lamination parameter were introduced by Miki,^{25,26} building upon the work of Tsai et al.,²⁷ with further notable contributions made by Fukunaga and Sekine.²⁸ Given any composite laminate composed of layers with identical material properties, the stacking sequence may be represented using a maximum of twelve lamination parameters, and no more than eight lamination parameters for mid-plane symmetric laminates, with further reductions possible through additional assumptions. The space of lamination parameters has been shown to be convex,²⁹ and as such they are commonly used in optimisation^{26,28,30} due to this simplified design space. Lamination parameters can, however, complicate the design process as they are not independent, but interrelated by complex relationships which define

feasible regions, a comprehensive review of which may be found in.³¹

In many uncertainty quantification techniques, the computational effort increases with the number of random variables, and as such it can be computationally expensive to model ply orientation uncertainty in composite laminates with a large number of plies. Scarth et al.³² used lamination parameters to represent ply orientation uncertainty as a small, fixed number of random variables regardless of the number of plies, in the uncertainty quantification of the aeroelastic stability of composite plate wings. To date, the use of lamination parameters to represent uncertainty has been limited to random variable models. In this paper, an approach is proposed for using lamination parameters to model random fields, in which the ply orientation uncertainty is defined using Karhunen-Loève Expansion, and the lamination parameters are approximated using an intrusive Polynomial Chaos Expansion. This approach is advantageous in that it preserves the separation of the random and spatial terms under the nonlinear transformation which defines the lamination parameters, while providing physical insight through closed-form expressions.

The paper is structured as follows. The lamination parameters are introduced in section II, Karhunen-Loève Expansion and Polynomial Chaos Expansion are introduced in section III. In section IV, closed-form expressions are derived for a PCE of the lamination parameters in a simple Gaussian distributed, random variable case study. These expressions are compared against closed-form expressions of the mean and variance, and Monte Carlo estimates of the Probability Density Functions (PDFs). In section V, the approach is extended to random fields, and compared against Monte Carlo estimates of the marginal distributions and covariance functions of the field.

II. Introduction to Lamination Parameters

A composite laminate composed of n plies, with i^{th} ply orientation denoted θ_i , is shown in Figure 1 along with the geometry and coordinate systems used in this paper.

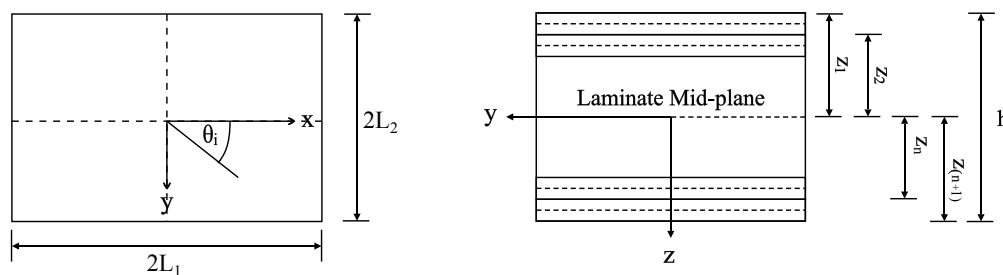


Figure 1: Composite laminate geometry and coordinate system.

In classical lamination theory,³³ applied in-plane stress resultants \mathbf{N} , and out-of-plane moment resultants \mathbf{M} , are related to mid-plane strains $\boldsymbol{\varepsilon}^0$, and curvatures $\boldsymbol{\kappa}$, by

$$\begin{Bmatrix} \mathbf{N} \\ \mathbf{M} \end{Bmatrix} = \begin{bmatrix} A & B \\ B & D \end{bmatrix} \begin{Bmatrix} \boldsymbol{\varepsilon}^0 \\ \boldsymbol{\kappa} \end{Bmatrix} \quad (1)$$

where A , B , and D are the laminate in-plane, extension-bending coupling, and out-of-plane stiffness matrices respectively. When using the lamination parameters,^{25,27} these stiffness matrices may be expressed as a linear function of the lamination parameters, material invariants and laminate thickness, given by

$$\begin{pmatrix} A_{11} \\ A_{12} \\ A_{22} \\ A_{66} \\ A_{16} \\ A_{26} \end{pmatrix} = h \begin{bmatrix} 1 & \xi_1^A & \xi_2^A & 0 & 0 \\ 0 & 0 & -\xi_2^A & 1 & 0 \\ 1 & -\xi_1^A & \xi_2^A & 0 & 0 \\ 0 & 0 & -\xi_2^A & 0 & 1 \\ 0 & \xi_3^A/2 & \xi_4^A & 0 & 0 \\ 0 & \xi_3^A/2 & -\xi_4^A & 0 & 0 \end{bmatrix} \begin{pmatrix} U_1 \\ U_2 \\ U_3 \\ U_4 \\ U_5 \end{pmatrix} \quad (2)$$

$$\begin{pmatrix} B_{11} \\ B_{12} \\ B_{22} \\ B_{66} \\ B_{16} \\ B_{26} \end{pmatrix} = \frac{h^2}{4} \begin{bmatrix} 1 & \xi_1^B & \xi_2^B & 0 & 0 \\ 0 & 0 & -\xi_2^B & 0 & 0 \\ 1 & -\xi_1^B & \xi_2^B & 0 & 0 \\ 0 & 0 & -\xi_2^B & 0 & 0 \\ 0 & \xi_3^B/2 & \xi_4^B & 0 & 0 \\ 0 & \xi_3^B/2 & -\xi_4^B & 0 & 0 \end{bmatrix} \begin{pmatrix} U_1 \\ U_2 \\ U_3 \\ U_4 \\ U_5 \end{pmatrix} \quad (3)$$

$$\begin{pmatrix} D_{11} \\ D_{12} \\ D_{22} \\ D_{66} \\ D_{16} \\ D_{26} \end{pmatrix} = \frac{h^3}{12} \begin{bmatrix} 1 & \xi_1^D & \xi_2^D & 0 & 0 \\ 0 & 0 & -\xi_2^D & 1 & 0 \\ 1 & -\xi_1^D & \xi_2^D & 0 & 0 \\ 0 & 0 & -\xi_2^D & 0 & 1 \\ 0 & \xi_3^D/2 & \xi_4^D & 0 & 0 \\ 0 & \xi_3^D/2 & -\xi_4^D & 0 & 0 \end{bmatrix} \begin{pmatrix} U_1 \\ U_2 \\ U_3 \\ U_4 \\ U_5 \end{pmatrix} \quad (4)$$

where h is the laminate thickness, and the material invariants U_i are defined in terms of the reduced lamina stiffnesses, Q_{ij} , as

$$\begin{pmatrix} U_1 \\ U_2 \\ U_3 \\ U_4 \\ U_5 \end{pmatrix} = \frac{1}{8} \begin{bmatrix} 3 & 2 & 3 & 4 \\ 4 & 0 & -4 & 0 \\ 1 & -2 & 1 & -4 \\ 1 & -6 & 1 & -4 \\ 1 & -1 & 2 & 4 \end{bmatrix} \begin{pmatrix} Q_{11} \\ Q_{12} \\ Q_{22} \\ Q_{66} \end{pmatrix} \quad (5)$$

which are in turn defined as

$$Q_{11} = E_{11}^2 / (E_{11} - E_{22}\nu_{12}^2) \quad (6)$$

$$Q_{22} = E_{11}E_{22} / (E_{11} - E_{22}\nu_{12}^2) \quad (7)$$

$$Q_{12} = \nu_{12}Q_{22} \quad (8)$$

$$Q_{66} = G_{12} \quad (9)$$

where E_{11} , E_{22} , G_{12} and ν_{12} are the longitudinal, transverse and shear moduli, and the Poisson's ratio respectively.

The lamination parameters are defined by the integrals

$$\xi_{[1,2,3,4]}^A = \frac{1}{2} \int_{-1}^1 \left[\cos(2\theta(u)), \cos(4\theta(u)), \sin(2\theta(u)), \sin(4\theta(u)) \right] du \quad (10)$$

$$\xi_{[1,2,3,4]}^B = \int_{-1}^1 \left[\cos(2\theta(u)), \cos(4\theta(u)), \sin(2\theta(u)), \sin(4\theta(u)) \right] u du \quad (11)$$

$$\xi_{[1,2,3,4]}^D = \frac{3}{2} \int_{-1}^1 \left[\cos(2\theta(u)), \cos(4\theta(u)), \sin(2\theta(u)), \sin(4\theta(u)) \right] u^2 du \quad (12)$$

where $\theta(u)$ is the distribution of the ply orientations with respect to normalised through-thickness coordinate $u = 2z/h$.

In practice, the integrals defined in Eqs. (10-12) reduce to finite summations of discrete, ply-level properties. For the sake of brevity, a 'general' lamination parameter ξ_k^l is used throughout this paper, which is defined using such a discrete sum, as

$$\xi_k^l = \frac{1}{2} \sum_{i=1}^n f(a\theta_i)(u_{i+1}^b - u_i^b) \quad (13)$$

where $k \in \{1, 2, 3, 4\}$, $l \in \{A, B, D\}$, and

$$a = \begin{cases} 2 & \text{if } k \in \{1, 3\} \\ 4 & \text{if } k \in \{2, 4\} \end{cases}, \quad b = \begin{cases} 1 & \text{if } l = A \\ 2 & \text{if } l = B \\ 3 & \text{if } l = D \end{cases} \quad (14)$$

and

$$f(x) = \begin{cases} \cos(x) & \text{if } k \in \{1, 2\} \\ \sin(x) & \text{if } k \in \{3, 4\} \end{cases} \quad (15)$$

where n is the number of plies and u_i denotes the normalised through-thickness coordinate of the upper surface of the i^{th} ply, noting that u_{n+1} denotes the coordinate of the lower surface of the laminate.

A maximum of twelve lamination parameters are required regardless of the number of plies. If the laminate is

mid-plane symmetric, ξ_{1-4}^B are zero and a total of eight parameters are required. If the laminate is balanced, ξ_{3-4}^A are eliminated and ξ_{3-4}^D are small and commonly ignored, while ξ_{3-4}^D may be eliminated entirely by using an anti-symmetric layup. Furthermore, it is common to restrict the plies to a discrete set of 0° , $\pm 45^\circ$, and 90° orientations, in which case $\xi_4^{A,B,D} = 0$.

III. Representation of Uncertainty

A. Karhunen-Loève Expansion

A random field, $H(\mathbf{x}, \omega)$, may be defined as a collection of random variables indexed by continuous spatial parameter $\mathbf{x} \in \mathcal{D}$, where spatial domain \mathcal{D} is an open set on \mathbb{R}^d which defines the geometry of the structure, and $\omega \in \Omega$ is a set of possible outcomes taken from the sample space Ω . At a given spatial coordinate, \mathbf{x}_0 , $H(\mathbf{x}_0, \omega)$ is a random variable, whereas for a given outcome, ω_0 , $H(\mathbf{x}, \omega_0)$ defines a deterministic realisation of the field.⁸ For practical applications it is necessary to discretise the field into a finite set of random variables, which is commonly achieved using Karhunen-Loève Expansion (e.g.^{6,19-22}).

Supposing that the random field is characterised by a symmetric and positive-definite covariance function, $C(\mathbf{x}, \mathbf{x}')$, it may be represented by spectral decomposition, and expressed as a generalised Fourier series as

$$H(\mathbf{x}, \omega) = H_0(\mathbf{x}) + \sum_{j=1}^{\infty} \sqrt{\lambda_j} \zeta_j(\omega) \varphi_j(\mathbf{x}) \quad (16)$$

where the $\zeta_j(\omega)$ form a set of uncorrelated random variables and $(\bullet)_0$ is used to denote the deterministic value of (\bullet) throughout this paper. If $H(\mathbf{x}, \omega)$ is a Gaussian random field, ζ_j are independent Gaussian random variables. The constants λ_j and functions $\varphi_j(\mathbf{x})$ correspond to the eigenvalues and eigenfunctions of the integral

$$\int_{\mathcal{D}} C(\mathbf{x}, \mathbf{x}') \varphi_j(\mathbf{x}) d\mathbf{x} = \lambda_j \varphi_j(\mathbf{x}') \quad \forall j = 1, 2, \dots \quad (17)$$

The eigenvalues may be sorted into a decreasing series converging upon zero, and as such it is possible to truncate the expansion after the m^{th} term to obtain a finite-dimensional approximation of the field. The KLE separates the randomness from the spatial dependency, and as such enables the spatial functions to be integrated directly into system matrices in subsequent analysis.

In this paper, a random field with exponentially decaying covariance function is assumed, which is defined as

$$C(\mathbf{x}, \mathbf{x}') = e^{-\|\mathbf{x} - \mathbf{x}'\|/c} \quad (18)$$

where c is the correlation length, a measure of the typical length-scale of variations. A small correlation length results in

a field which varies substantially over small distances, tending to white noise as c approaches zero. Conversely, a large correlation length results in a field which does not vary significantly over the spatial domain, tending towards a random variable as c approaches infinity. Modelling a random field with small correlation length typically requires a greater number of KLE terms, consequentially increasing the dimensionality of the problem. For an exponential covariance function, a closed-form solution of the eigenvalue problem in Eq. (17) may be found in.⁶ Using this expression, example realisations of a one-dimensional random field are shown for different correlation lengths in Figure 2.

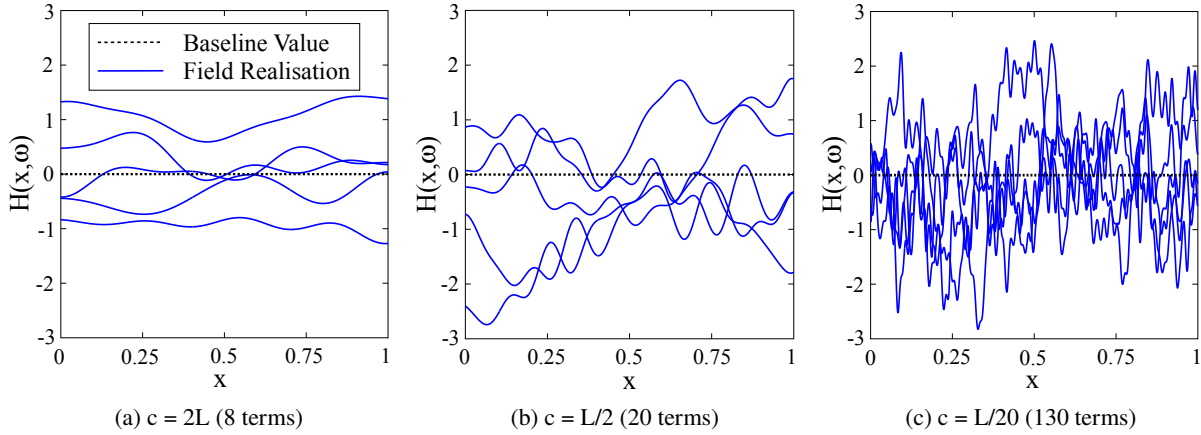


Figure 2: Example random field realisations obtained using Karhunen-Loève Expansion

B. Polynomial Chaos Expansion

Polynomial Chaos Expansion is commonly used to propagate parametric uncertainty through mathematical models (e.g.^{12,20,22,32}). In this approach, a second-order stochastic process, $X(\omega)$, is represented as a series of orthogonal polynomials in a set of basic random variables, expressed as^{6,7}

$$\begin{aligned}
 X(\omega) = & a_0 \Gamma_0 + \sum_{i_1=1}^{\infty} a_{i_1} \Gamma_1(\zeta_{i_1}(\omega)) + \sum_{i_1=1}^{\infty} \sum_{i_2=1}^{i_1} a_{i_1 i_2} \Gamma_2(\zeta_{i_1}(\omega), \zeta_{i_2}(\omega)) \\
 & + \sum_{i_1=1}^{\infty} \sum_{i_2=1}^{i_1} \sum_{i_3=1}^{i_2} a_{i_1 i_2 i_3} \Gamma_3(\zeta_{i_1}(\omega), \zeta_{i_2}(\omega), \zeta_{i_3}(\omega)) + \dots
 \end{aligned} \tag{19}$$

where a_{i_1, \dots, i_p} are deterministic coefficients, and $\Gamma_p(\zeta_{i_1}, \dots, \zeta_{i_p})$ is the polynomial chaos of order p in multivariate random variable $\zeta = \{\zeta_{i_1}, \dots, \zeta_{i_p}\}$. If ζ is composed of independent, standard Gaussian variables, the Γ_p terms are given by the Hermite polynomials, which are defined as

$$H_p(\zeta_{i_1}, \dots, \zeta_{i_p}) = (-1)^p \frac{\partial e^{-\frac{1}{2}\zeta^T \zeta}}{\partial \zeta_{i_1}, \dots, \partial \zeta_{i_p}} e^{\frac{1}{2}\zeta^T \zeta} \tag{20}$$

If the random variables are non-Gaussian, the polynomial chaos may be formed of a different set of orthogonal polynomials depending on the input distribution and its support. For example, Legendre polynomials may be used for

uniformly distributed inputs, or Laguerre polynomials for gamma distributed variables.⁷ For notational convenience, Eq. (19) is often more concisely written as

$$X(\omega) = \sum_{j=0}^{\infty} \hat{a}_j \Psi_j(\zeta(\omega)) \quad (21)$$

where there is a one-to-one correspondence between $\Gamma_p(\zeta_{i_1}, \dots, \zeta_{i_p})$ and $\Psi_j(\zeta)$, as well as a_{i_1, \dots, i_p} and \hat{a}_j . The polynomials, $\Psi_j(\omega)_{j=1}^{\infty}$, form a complete orthogonal basis with respect to ζ , and can therefore guarantee exponential convergence with increasing polynomial order, as well as possessing the following useful properties

$$\Psi_0 = 1 \quad (22)$$

$$\mathbb{E}[\Psi_j(\omega)] = 0 \quad (23)$$

$$\mathbb{E}[\Psi_j(\omega)\Psi_k(\omega)] = \delta_{jk}\mathbb{E}[\Psi_j(\omega)^2] \quad (24)$$

where δ_{jk} is the Kronecker delta, defined as

$$\delta_{jk} = \begin{cases} 1 & \text{if } j = k \\ 0 & \text{otherwise} \end{cases} \quad (25)$$

and $\mathbb{E}[\zeta]$ denotes the expectation operator, which is evaluated as

$$\int_S \zeta f(\zeta) d\zeta \quad (26)$$

where S is the support of random variable ζ , defined in \mathbb{R}^n , where n is the dimension of the random variable.

In practice, Eq. (21) is truncated to P terms, which introduces an error. The unknown coefficients may be determined by minimising this error in a mean-square sense, which is equivalent to setting the residual as orthogonal to the basis polynomials. Supposing the expansion represents random vector \mathbf{y} , this condition may be expressed as

$$\mathbb{E} \left[\left(\mathbf{y} - \sum_{j=0}^{P-1} \hat{\mathbf{a}}_j \Psi_j(\omega) \right) \Psi_k(\omega) \right] = 0, \quad \forall k = 0, \dots, P-1 \quad (27)$$

Due to the orthogonality of polynomials, Eq. (27) is simplified, and the vector-valued coefficients are given by

$$\hat{\mathbf{a}}_j = \frac{\mathbb{E}[\mathbf{y}(\omega)\Psi_j(\omega)]}{\mathbb{E}[\Psi_j(\omega)^2]} \quad (28)$$

In an intrusive Polynomial Chaos Expansion, closed form expressions are sought for the numerator of Eq. (28). The denominator is a normalising coefficient, the calculation of which is trivial. Realisations of \mathbf{y} may be simulated using

the basis functions, $\Psi_j(\omega)$, and the mean vector and covariance matrix may be determined as

$$\mathbb{E}[\mathbf{y}(\omega)] = \hat{\mathbf{a}}_0 \quad (29)$$

$$\text{cov}[\mathbf{y}(\omega), \mathbf{y}(\omega)] = \sum_{j=1}^{P-1} \mathbb{E}[\Psi_j(\omega)^2] \hat{\mathbf{a}}_j \hat{\mathbf{a}}_j^T \quad (30)$$

In this paper, the outlined approach is used to approximate the distributions of all twelve lamination parameters, grouped together as a vector, $\boldsymbol{\xi} = \{\xi_1^A, \dots, \xi_4^D\}^T$. In the subsequent sections, two cases are presented in which the ply orientations are modelled as Gaussian random variables, and random fields respectively.

IV. Uncertainty Modelling Using Random Variables

A. Intrusive Expansion for the Lamination Parameters

In this section, closed-form expressions are derived for the coefficients of an intrusive Polynomial Chaos Expansion for the lamination parameters. These coefficients are twelve-dimensional vectors with a component corresponding to each lamination parameter. For the sake of brevity, full derivations are included only for the first component of each vector, which corresponds to ξ_1^A , before general expressions are presented for the ‘general’ lamination parameter introduced in Section II.

The ply orientations are assumed to be Gaussian distributed random variables. For use in a Polynomial Chaos Expansion, it is necessary to define these ply orientations as a function of standard Gaussian variables with zero mean and unit variance, which may be expressed as

$$\theta_i(\omega) = \theta_{i0} + \sigma \zeta_i(\omega) \quad (31)$$

where θ_{i0} is the deterministic orientation of the i^{th} ply, $\zeta_i(\omega)$ is a standard Gaussian random variable, and σ is the standard deviation of the ply orientations. The intrusive expansion requires that closed-form expressions are obtained for the expectation in the numerator of Eq. (28). Using Eq. (13) this expectation may be written for ξ_1^A as

$$\mathbb{E}[\xi_1^A(\omega) \Psi_j(\omega)] = \frac{1}{2} \int_{-\infty}^{\infty} \dots \int_{-\infty}^{\infty} \left(\sum_{i=1}^n \cos(2\theta_i(\omega)) (u_{i+1} - u_i) \right) \Psi_j(\omega) \phi(\boldsymbol{\zeta}) d\zeta_1, \dots, d\zeta_n \quad (32)$$

where $\phi(\boldsymbol{\zeta})$ is the multivariate Gaussian PDF and n is the number of plies. The $\Psi_j(\omega)$ terms are multivariate polynomials in $\boldsymbol{\zeta}$, which may be expanded as the product of n univariate Hermite polynomials $H_p(\zeta_j)$ using

$$\Psi_j(\omega) = \prod_{i=1}^n H_{\alpha_{ij}}(\zeta_i(\omega)) \quad (33)$$

where α_{ij} is an element of a multi-index which governs the order of the i^{th} univariate polynomial in the j^{th} basis function. This multi-index is defined as

$$\boldsymbol{\alpha}_j = \{\alpha_{1j}, \dots, \alpha_{nj}\}, \quad \text{where } \alpha_{ij} \in \{0, 1, \dots, p\}, \quad \text{subject to } \sum_{i=1}^n \alpha_{ij} \leq p \quad (34)$$

where p is the maximum total order of the polynomials. Expanding the basis polynomials and exploiting the independence of the random variables, Eq. (32) may be expanded as

$$\mathbb{E}[\xi_1^A(\omega)\Psi_j(\omega)] = \frac{1}{2} \sum_{i=1}^n (u_{i+1} - u_i) \int_{-\infty}^{\infty} H_{\alpha_{ij}}(\zeta_i) \cos(2\theta_i(\omega)) \phi(\zeta_i) d\zeta_i \prod_{k=1, k \neq i}^n \int_{-\infty}^{\infty} H_{\alpha_{kj}}(\zeta_k) \phi(\zeta_k) d\zeta_k \quad (35)$$

Using Eq. (23), it can be seen that Eq. (35) is zero in all cases in which more than one of the α_{ij} terms is greater than zero, and is otherwise given by

$$\mathbb{E}[\xi_1^A(\omega)\Psi_j(\omega)] = \begin{cases} \frac{1}{2} \sum_{i=1}^n (u_{i+1} - u_i) \int_{-\infty}^{\infty} \cos(2\theta_i(\omega)) \phi(\zeta_i) d\zeta_i & \text{if } \alpha_{ij} = 0 \forall i \\ \frac{1}{2} (u_{i+1} - u_i) \int_{-\infty}^{\infty} H_{\alpha_{ij}}(\zeta_i) \cos(2\theta_i(\omega)) \phi(\zeta_i) d\zeta_i & \text{otherwise} \end{cases} \quad (36)$$

The cases in which multiple of the α_{ij} are greater than zero, correspond to polynomials which capture the effects of the interaction between uncertainty in different ply orientations. The above observation indicates that due to the orthogonality of the polynomials, these interactions are all zero. Similar properties are exhibited by all orthogonal polynomials in the Askey scheme, and as such, this observation is also true for non-Gaussian distributed ply orientations. It is therefore possible to express the PCE as a weighted sum of univariate orthogonal polynomials, summed over all of the plies of the laminate. As such, the number of random variables scales linearly with the number of plies.

Substituting Eq. (31) into the first case of Eq. (36), along with the definition of the Gaussian distribution, the first term of the expansion may be evaluated as

$$\begin{aligned} \mathbb{E}[\xi_1^A(\omega)\Psi_0(\omega)] &= \frac{1}{2\sqrt{2\pi}} \sum_{i=1}^n (u_{i+1} - u_i) \int_{-\infty}^{\infty} \cos(2\theta_{i0} + 2\sigma\zeta_i) e^{-\frac{1}{2}\zeta_i^2} d\zeta_i \\ &= \frac{1}{2\sqrt{2\pi}} \sum_{i=1}^n (u_{i+1} - u_i) \int_{-\infty}^{\infty} (\cos(2\theta_{i0}) \cos(2\sigma\zeta_i) - \sin(2\theta_{i0}) \sin(2\sigma\zeta_i)) e^{-\frac{1}{2}\zeta_i^2} d\zeta_i \\ &= \frac{1}{2} e^{-2\sigma^2} \sum_{i=1}^n (u_{i+1} - u_i) \cos(2\theta_{i0}) = e^{-2\sigma^2} \xi_{10}^A \end{aligned} \quad (37)$$

The $\sin(2\sigma\zeta_i)$ term originates from the application of the compound angle formula to Eq. (31), and is eliminated from the integral due to symmetry. The first expansion coefficient is therefore given by the deterministic lamination parameter value, denoted ξ_{10}^A , scaled by a factor which decreases exponentially with the ply orientation variance.

A similar process is used to determine the remaining coefficients of the expansion, which are given by the second

case of Eq. (36). The compound angle formulae is applied as above, and due to symmetry the $\cos(2\sigma\zeta_j)$ and $\sin(2\sigma\zeta_j)$ terms are eliminated for the coefficients corresponding to odd and even polynomials respectively. The coefficients therefore have different values for odd and even j , which can be shown to be given by

$$\begin{aligned} \mathbb{E}[\xi_1^A(\omega)H_j(\zeta_i(\omega))] &= \frac{1}{2\sqrt{2\pi}}(u_{i+1} - u_i) \int_{-\infty}^{\infty} (\cos(2\theta_{i0}) \cos(2\sigma\zeta_i) - \sin(2\theta_{i0}) \sin(2\sigma\zeta_i)) e^{-\frac{\zeta_i^2}{2}} H_j(\zeta_i) d\zeta_i \\ &= \begin{cases} -(u_{i+1} - u_i) \sin(2\theta_{i0}) \sigma (-4\sigma^2)^{\frac{j-1}{2}} e^{-2\sigma^2} & \text{if } j \text{ is odd} \\ \frac{1}{2}(u_{i+1} - u_i) \cos(2\theta_{i0}) (-4\sigma^2)^{\frac{j}{2}} e^{-2\sigma^2} & \text{if } j \text{ is even} \end{cases} \end{aligned} \quad (38)$$

It is also necessary to determine the normalising factor given by the denominator of Eq. (28). For univariate Hermite polynomials, it can be shown that this factor is given by

$$\mathbb{E}[H_j(\zeta_i(\omega))^2] = j! \quad (39)$$

The complete Polynomial Chaos Expansion is therefore given by

$$\begin{aligned} \xi_1^A(\omega) &\approx e^{-2\sigma^2} \left(\xi_{10}^A - \frac{1}{2} \sum_{j=1}^{\lfloor \frac{p+1}{2} \rfloor} \frac{2\sigma(-4\sigma^2)^{j-1}}{(2j-1)!} \sum_{i=1}^n (u_{i+1} - u_i) \sin(2\theta_{i0}) H_{2j-1}(\zeta_i(\omega)) \right. \\ &\quad \left. + \frac{1}{2} \sum_{j=1}^{\lfloor \frac{p}{2} \rfloor} \frac{(-4\sigma^2)^j}{(2j)!} \sum_{i=1}^n (u_{i+1} - u_i) \cos(2\theta_{i0}) H_{2j}(\zeta_i(\omega)) \right) \end{aligned} \quad (40)$$

where $\lfloor \bullet \rfloor$ denotes the floor operator, which rounds down to the nearest integer. Noting that the PCE described in Section B is used to represent a twelve-dimensional vector of lamination parameters, the above analysis can be repeated to obtain the component of this vector corresponding to ‘general’ lamination parameter, ξ_k^l , as

$$\begin{aligned} \xi_k^l(\omega) &\approx e^{-\frac{1}{2}a^2\sigma^2} \left(\xi_{k0}^l + \frac{1}{2} \sum_{j=1}^{\lfloor \frac{p+1}{2} \rfloor} \frac{a\sigma(-a^2\sigma^2)^{j-1}}{(2j-1)!} \sum_{i=1}^n (u_{i+1}^b - u_i^b) g(a\theta_{i0}) H_{2j-1}(\zeta_i(\omega)) \right. \\ &\quad \left. + \frac{1}{2} \sum_{j=1}^{\lfloor \frac{p}{2} \rfloor} \frac{(-a^2\sigma^2)^j}{(2j)!} \sum_{i=1}^n (u_{i+1}^b - u_i^b) f(a\theta_{i0}) H_{2j}(\zeta_i(\omega)) \right) \end{aligned} \quad (41)$$

where a, b, f, k and l are as defined in relation to Eq. (13), and

$$g(x) = \begin{cases} -\sin(x) & \text{if } k \in \{1, 2\} \\ \cos(x) & \text{if } k \in \{3, 4\} \end{cases} \quad (42)$$

The basis functions $H_j(\zeta_i(\omega))$ are shared between all components of the vector, and may be used to simulate realisations of the lamination parameters. By using the proposed approach, a set of n ply orientations are instead represented using

a set of $n \times p$ random variables. The number of variables is by definition greater than or equal to the number of ply orientations, and as such, this formulation is not a useful representation of the uncertainty.

B. Statistical Properties of the Lamination Parameters

1. Overview

In the following sections, numerical results are obtained using the expansions derived in the previous section, and are compared against results for the lamination parameters themselves. Exact closed-form expressions are derived for the mean and variance, and are compared against polynomial chaos approximations. Emulated PDFs are subsequently compared against Monte Carlo Simulation results for lamination parameters corresponding to various layups. To the knowledge of the authors, there is very little experimental data available for the statistical properties of the ply orientations, which depend not only upon the material, but also the manufacturing process. As such, throughout this paper, numerical results are obtained for a range of standard deviations of 1° , 2.5° , and 5° , in order to investigate changes in behaviour with different assumptions. The large value of 5° is chosen to highlight errors when modelling larger deviations in ply orientations.

2. Exact Closed-Form Expressions

In this section, closed form expressions are derived for the mean, variance, and covariance of the lamination parameters. For the sake of brevity, full derivations are only included for the variance of ξ_1^A , and covariance of ξ_1^A with ξ_2^A . In each case the ply orientations are assumed to be Gaussian distributed, as expressed in Eq. (31).

As the expectation of a sum is equal to the sum of expectations, it is trivial to show that the mean of general lamination parameter ξ_k^l , is given by

$$\mathbb{E}[\xi_k^l(\omega)] = \frac{1}{2} e^{-\frac{1}{2}a^2\sigma^2} \sum_{i=1}^n (u_{i+1}^b - u_i^b) f(a\theta_{i0}) = e^{-\frac{1}{2}a^2\sigma^2} \xi_{k0}^l \quad (43)$$

which is identical to the first term of the Polynomial Chaos Expansion in Eq. (41). By using the well-known Bienaymé formula, the variance of a sum may be expanded as the sum of variances, and the variance of ξ_1^A expanded as

$$\begin{aligned} \text{Var}[\xi_1^A(\omega)] &= \text{Var} \left[\frac{1}{2} \sum_{i=1}^n (u_{i+1} - u_i) \cos(2\theta_{i0} + 2\sigma\zeta_i(\omega)) \right] \\ &= \frac{1}{4} \sum_{i=1}^n (u_{i+1} - u_i)^2 (\mathbb{E}[\cos^2(2\theta_{i0} + 2\sigma\zeta_i(\omega))] - \mathbb{E}[\cos(2\theta_{i0} + 2\sigma\zeta_i(\omega))]^2) \end{aligned} \quad (44)$$

Using the fact that $\cos^2(2\theta) = \frac{1}{2}(1 + \cos(4\theta))$, and exploiting the trends in expectation noted in Eq. (43), the

expectations in Eq. (44) may be evaluated to give the variance as

$$\text{Var}[\xi_1^A(\omega)] = \frac{1}{8} \sum_{i=1}^n (u_{i+1} - u_i)^2 (1 - e^{-4\sigma^2} - \cos(4\theta_{i0})e^{-4\sigma^2} + \cos(4\theta_{i0})e^{-8\sigma^2}) \quad (45)$$

A similar approach may be used to determine the covariance between ξ_1^A and ξ_2^A , which is first expressed as

$$\begin{aligned} \text{cov}[\xi_1^A(\omega), \xi_2^A(\omega)] &= \frac{1}{4} \sum_{i=1}^n (u_{i+1} - u_i)^2 (\mathbb{E}[\cos(2\theta_{i0} + 2\sigma\zeta_i(\omega)) \cos(4\theta_{i0} + 4\sigma\zeta_i(\omega))] \\ &\quad - \mathbb{E}[\cos(2\theta_{i0} + 2\sigma\zeta_i(\omega))] \mathbb{E}[\cos(4\theta_{i0} + 4\sigma\zeta_i(\omega))]) \end{aligned} \quad (46)$$

and using the fact that $\cos(2\theta)\cos(4\theta) = \cos(6\theta + 2\theta)$, as well as the previously noted trends in expectation, the covariance is evaluated as

$$\text{cov}[\xi_1^A(\omega), \xi_2^A(\omega)] = \frac{e^{-2\sigma^2}}{8} \sum_{i=1}^n (u_{i+1} - u_i)^2 (\cos(2\theta_{i0})(1 - e^{-8\sigma^2}) + \cos(6\theta_{i0})(e^{-16\sigma^2} - e^{-8\sigma^2})) \quad (47)$$

In a similar fashion, a general covariance term may be obtained as

$$\begin{aligned} \text{cov}[\xi_{k_1}^{l_1}(\omega), \xi_{k_2}^{l_2}(\omega)] &= \frac{1}{8} e^{-\frac{1}{2}(a_2 - a_1)^2 \sigma^2} (1 - e^{-a_1 a_2 \sigma^2}) \\ &\times \sum_{i=1}^n (u_{i+1}^{b_1} - u_i^{b_1})(u_{i+1}^{b_2} - u_i^{b_2}) \left(f((a_2 - a_1)\theta_{i0}) + (-1)^c f((a_2 + a_1)\theta_{i0}) e^{-a_1 a_2 \sigma^2} \right) \end{aligned} \quad (48)$$

where a_1 , a_2 , b_1 and b_2 are defined as in Eq. (14) using the values of k_1 , k_2 , l_1 and l_2 respectively, and

$$c = \begin{cases} 0 & \text{if } k_1 \in \{3, 4\} \text{ and } k_2 \in \{3, 4\} \\ 1 & \text{otherwise} \end{cases} \quad (49)$$

and $f(x)$ is redefined as

$$f(x) = \begin{cases} \sin(x) & \text{if } k_1 \in \{1, 2\} \text{ and } k_2 \in \{3, 4\}, \text{ or } k_1 \in \{3, 4\} \text{ and } k_2 \in \{1, 2\} \\ \cos(x) & \text{otherwise} \end{cases} \quad (50)$$

The above closed-form expressions section are now used to investigate trends with varying ply orientation, θ , in a number of parameterised layups. Assuming a ply orientation standard deviation of 2.5° . Trends in the mean and standard deviation of the out-of-plane lamination parameters of a single ply laminate, $[\theta]$, a two-ply anti-symmetric laminate $[\theta, -\theta]$, and a four-ply symmetric laminate $[\theta, -\theta]_S$ are shown in Figures 3 and 4 respectively.

The mean trends in Figure 3 simply follow deterministic trends in the lamination parameters, weighted by a

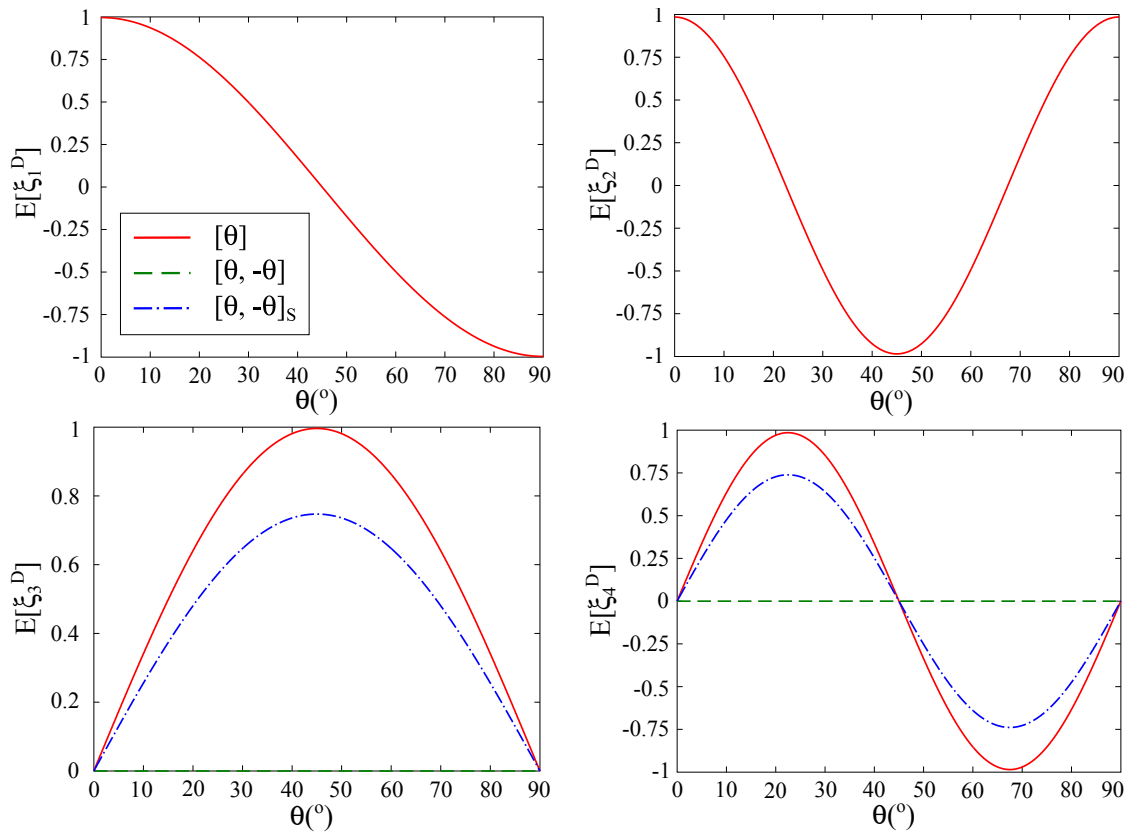


Figure 3: Trends in the out-of-plane lamination parameter mean with varying ply orientation

factor which decreases exponentially with the ply orientation variance. The plots for ξ_1^D and ξ_2^D are identical for all parameterisations demonstrating that the mean is not affected by the number of plies. As in a deterministic laminate, the mean of ξ_3^D and ξ_4^D which govern bend-twist coupling, reduces with the number of plies in a balanced laminate such as the $[\theta, -\theta]_S$ example, and is zero for the anti-symmetric laminate.

The plots in Figure 4 follow weighted curves of $1 - \cos(4\theta)$, $1 - \cos(8\theta)$, $1 + \cos(4\theta)$ and $1 + \cos(8\theta)$, for ξ_{1-4}^D respectively. For all values of θ , the standard deviation decreases with an increasing number of plies due an averaging effect in which uncertainty in the different plies cancel each other out. The standard deviation varies considerably with the layup, and plots such as those in Fig 4 may be used to gain insight into how to tailor composite laminates to be less sensitive to uncertainty. For example, the bending stiffness D_{11} is maximised by 0° plies with $\xi_1^D = 1$, which can also be seen to minimise the variability in ξ_1^D . The torsional stiffness, D_{66} , is maximised by $\pm 45^\circ$ plies with $\xi_2^D = -1$, which also minimises variability in ξ_2^D , however, this also maximises the variability in ξ_1^D and therefore the bending stiffness. Bend-twist coupling, which is governed by ξ_{3-4}^D , is often undesirable, however, minimising ξ_3^D by using 0° and 90° plies results in maximising the variability in this parameter. It should also be noted that standard deviations of ξ_{3-4}^D for the anti-symmetric example follow the same trends as the other laminates, despite the fact that bend-twist coupling is eliminated in a deterministic analysis of such laminates.

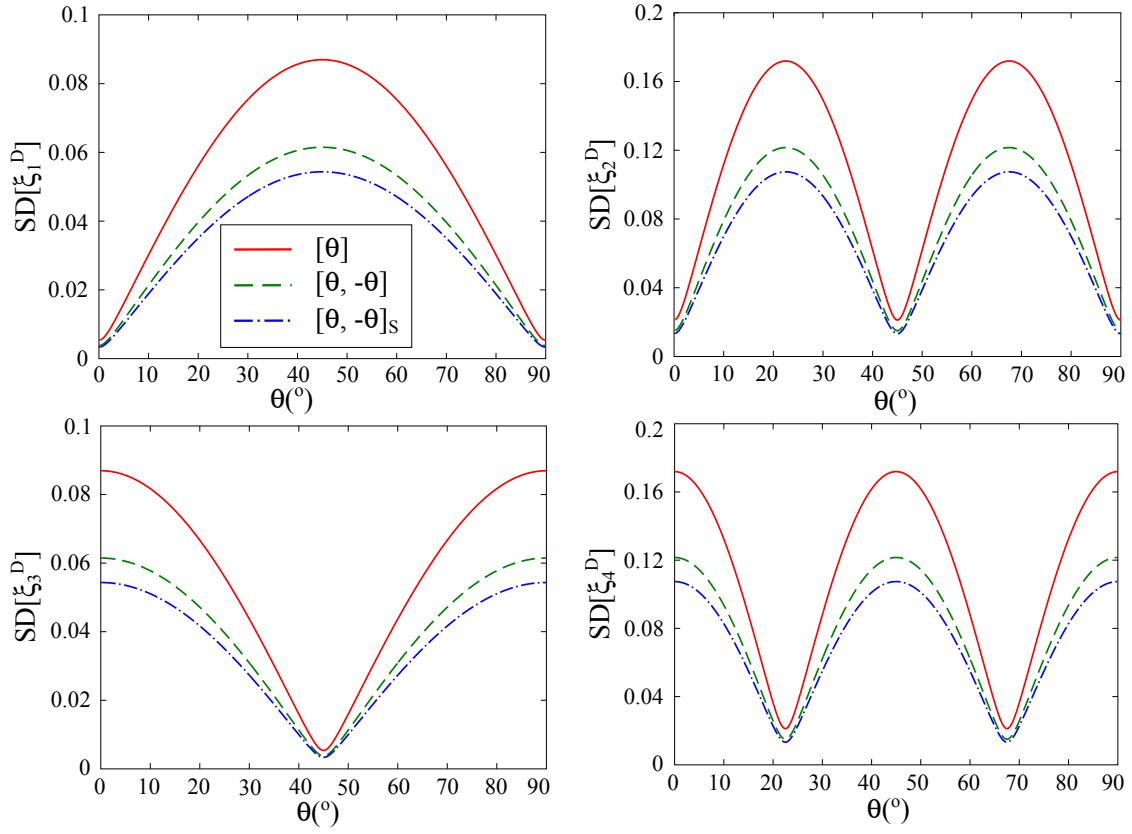


Figure 4: Trends in the out-of-plane lamination parameter standard deviation with varying ply orientation

3. Polynomial Chaos Expansion Approximations

In the previous section, a closed-form expression was derived for a general lamination parameter covariance term. In this section, example PCE approximations of the lamination parameter variance and covariance are derived and used to investigate the convergence of the expansion with increasing order.

The Polynomial Chaos Expansion approximation of the variance of ξ_1^A may be obtained using Eq. (30). By squaring each of the expansion coefficients and using the double angle formulae, along with the result of Eq. (39), the alternating series of sin and cos terms in Eq. (40) simplifies to a series of cos terms, to give the variance as

$$\text{Var}[\xi_1^A(\omega)] \approx \frac{e^{-4\sigma^2}}{8} \sum_{j=1}^p \frac{(4\sigma^2)^j}{(j!)} \sum_{i=1}^n (u_{i+1} - u_i)^2 (1 + (-1)^j \cos(4\theta_{i0})) \quad (51)$$

Noting that the Taylor series definition of the exponential function is given by

$$e^x = \sum_{i=0}^{\infty} \frac{x^i}{i!} \quad (52)$$

as the order of the Polynomial Chaos Expansion tends to infinity, Eq. (51) converges to

$$\text{Var}[\xi_1^A](\omega) = \frac{e^{-4\sigma^2}}{8} \sum_{i=1}^n (u_{i+1} - u_i)^2 (e^{4\sigma^2} - 1 + (e^{-4\sigma^2} - 1) \cos 4\theta_{i0}) \quad (53)$$

which can be seen through basic algebra to be identical to Eq. (45), and as such the Polynomial Chaos approximation of the variance converges towards the true value with increasing expansion order.

In a similar analysis, Polynomial Chaos Expansion may be used to approximate the covariance of ξ_1^A and ξ_2^A as

$$\begin{aligned} \text{cov}[\xi_1^A(\omega), \xi_2^A(\omega)] &\approx \frac{e^{-10\sigma^2}}{4} \left(\sum_{j=1}^{\lfloor \frac{p+1}{2} \rfloor} \frac{(8\sigma)^{2j-1}}{((2j-1)!)^2} \sum_{i=1}^n (u_{i+1} - u_i)^2 \sin(2\theta_{i0}) \sin(4\theta_{i0}) E[H_{2j-1}(\omega)^2] \right. \\ &\quad \left. + \sum_{j=1}^{\lfloor \frac{p}{2} \rfloor} \frac{(8\sigma)^{2j}}{((2j)!)^2} \sum_{i=1}^n (u_{i+1} - u_i)^2 \cos(2\theta_{i0}) \cos(4\theta_{i0}) E[H_{2j}(\omega)^2] \right) \\ &= \frac{e^{-10\sigma^2}}{8} \sum_{j=1}^p \frac{(8\sigma)^j}{j!} \sum_{i=1}^n (u_{i+1} - u_i)^2 (\cos(2\theta_{i0}) + (-1)^j \cos(6\theta_{i0})) \end{aligned} \quad (54)$$

As in the previous example, using the Taylor series definition of the exponential function, it is possible to show that this expression converges to that expressed in Eq. (47) as the expansion order tends to infinity.

In order to further investigate the convergence of the PCE, Figure 5 shows estimates of the standard deviation of the out-of-plane lamination parameters of a $[0, 90, \pm 45]_S$ laminate with increasing expansion order, alongside the natural log of the error relative to the closed-form solution from Eq. (48).

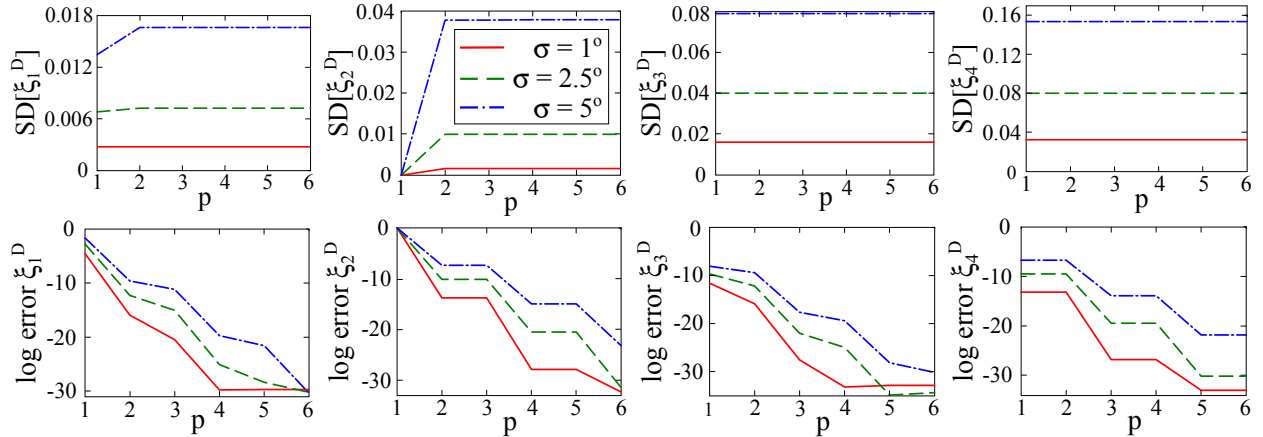


Figure 5: Convergence of out-of-plane lamination parameter standard deviation for a $[0, 90, \pm 45]_S$ laminate, with different values of ply orientation standard deviation

A good agreement is achieved between the Polynomial Chaos and closed-form expressions of the standard deviation for relatively low expansion order, with the relative error decreasing on an exponential scale for increasing order. An accurate approximation is achieved for ξ_{3-4}^D using a 1st order expansion, which suggests that these parameters are approximately Gaussian, whereas a 2nd order expansion is required for ξ_{1-2}^D . From Eq. (41), it can be seen that the

1st order coefficients of the PCE for ξ_2^D are factored by $\sin(4\theta_{i0})$, which are zero for orientations of 0° , $\pm 45^\circ$, and 90° . It is therefore possible to reduce the number of parameters by making restrictions to the layup, as is the case for a deterministic analysis. It is for this reason that a minimum 2nd order expansion is required to model these parameters, and for the stepped convergence in error which is especially notable for ξ_2^D . It can also be noted that the relative error is higher for the examples with a larger ply orientation standard deviation, and as such, higher order expansions may be required to model such behaviour.

4. Simulation of the Lamination Parameters

In this section, the proposed approach is used to estimate lamination parameter PDFs, which are compared with results of a Monte Carlo Simulation. PDFs for the out-of-plane lamination parameters of a $[0, 90, \pm 45]_S$ laminate are shown in Figure 6, assuming a ply orientation standard deviation of 2.5° . In order to compare the PDFs of the in-plane, extension-bending coupling, and out-of-plane lamination parameters, a similar exercise is undertaken for the PDFs of ξ_2^A , ξ_2^B and ξ_2^D of a $[0]_8$ laminate in Figure 7, assuming a ply orientation standard deviation of 5° so as to investigate convergence with a larger magnitude of uncertainty. Additionally, scatter plots of different sets of out-of-plane lamination parameters are shown in Figure 8 for the 4th order PCE of a $[0_2, 90_2]_S$ laminate, in order to investigate the ability to model correlated behaviour.

The results in Figure 6 reflect observations made in the previous section in relation to the $[0, 90, \pm 45]_S$ laminate, in that the PDFs of ξ_{3-4}^D are approximately Gaussian, and as such, a 1st order expansion is sufficient to model these parameters. The convergence with increasing order is most evident for ξ_1^D , in which a substantial improvement is achieved in using a 2nd order in favour of a 1st order expansion. In general, a 2nd order expansion is adequate to model all of the behaviour in this example. As discussed previously, some of the expansion coefficients are zero due to a dependency on $\sin(4\theta_{i0})$, and as such, plots corresponding to these coefficients are omitted from Figure 6.

Odd-valued expansions are omitted from Figure 7, as these depend upon $\sin(2\theta_{i0})$ which is zero for 0° plies. As in the previous case, a 2nd order expansion provides a reasonable agreement with the Monte Carlo results, however, a small improvement is achieved by using a 4th order expansion. This higher required order may be attributed to the higher standard deviation used for the ply orientations. The requirement of a 4th order expansion for the highest accuracy may also be attributed to the fact that the 3rd order coefficients are zero, however, this result also means that the 4th order expansion only requires two sets of coefficients. As such, it is difficult to make general statements regarding the required expansion order and number of expansion coefficients, as these depend upon the layup.

Finally, from Figure 8 it can be seen that the out-of-plane lamination parameters of the $[0_2, 90_2]_S$ laminate are highly correlated, and that this correlation is non-Gaussian. The 4th order Polynomial Chaos Expansion used in the example can be seen to give a good description of this correlation.

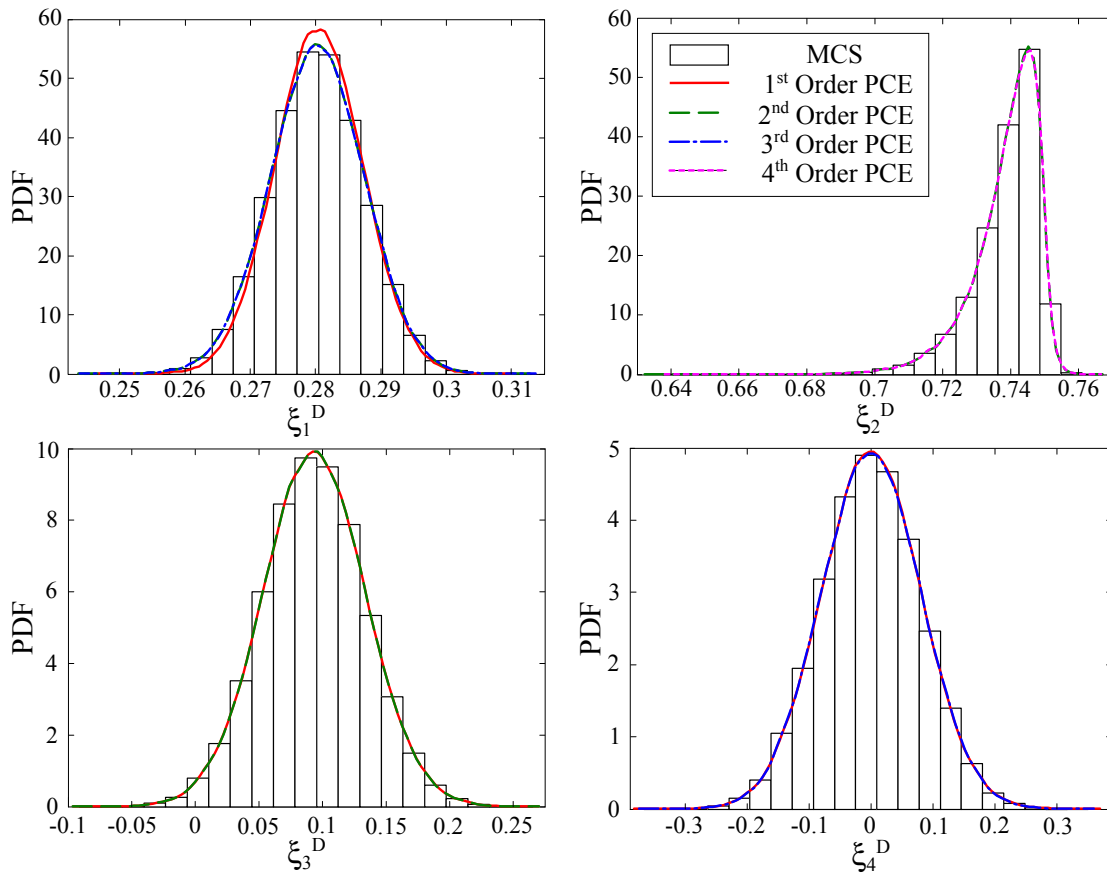


Figure 6: Convergence of out-of-plane lamination parameter PDFs for a $[0, 90, \pm 45]_S$ laminate

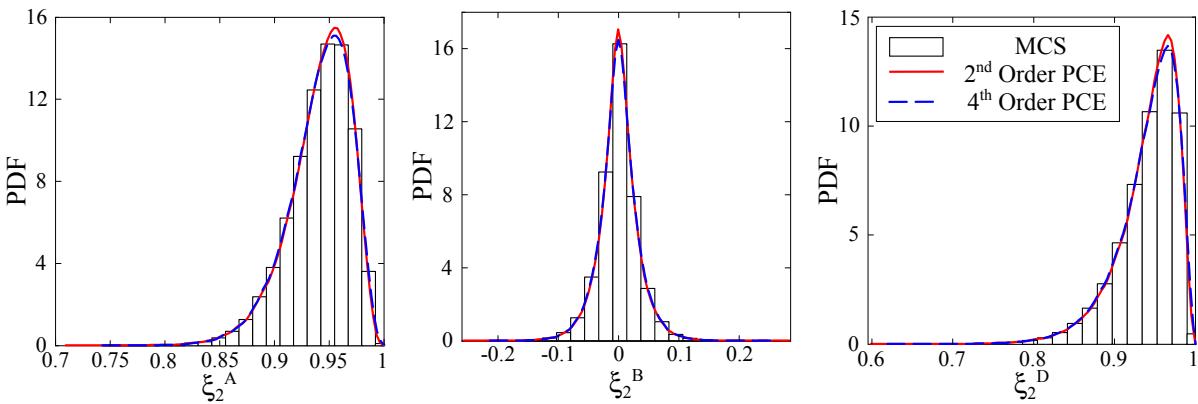


Figure 7: Convergence of in-plane, coupling, and out-of-plane lamination parameter PDFs for a $[0]_8$ laminate

V. Uncertainty Modelling Using Random Fields

A. Intrusive Expansion for Spatially Varying Lamination Parameters

Closed-form expressions are derived for the coefficients of a Polynomial Chaos Expansion for the lamination parameters, in which the ply orientations are modelled as Gaussian random fields. The analysis follows the approach taken in the random variable case study, with the ply orientations initially defined using a Karhunen-Loève Expansion. It should be

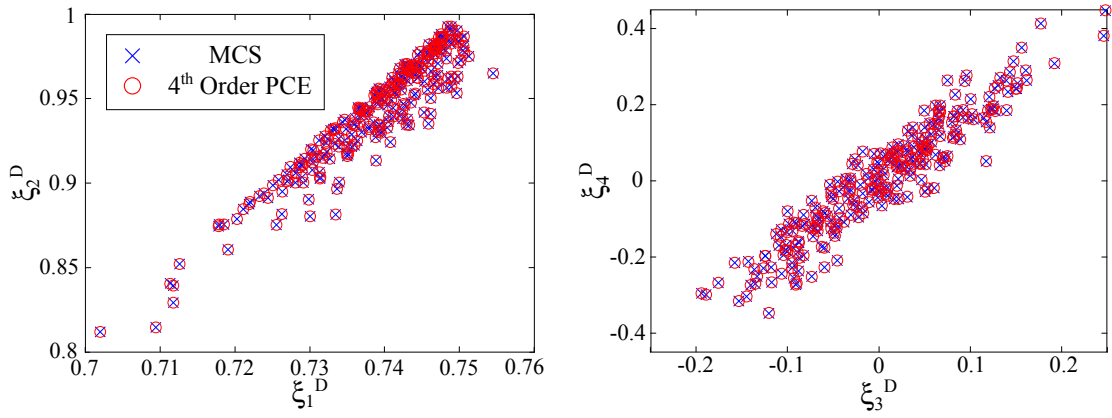


Figure 8: Comparison of scatter plots for the out-of-plane lamination parameters of a $[0_2, 90_2]_S$ laminate

noted that such an approach is only valid for Gaussian random fields. To extend the approach to non-Gaussian fields, it would be necessary to undertake a nonlinear transformation in order to target the non-Gaussian marginal distributions and covariance function.^{23,24,34,35}

Using a Karhunen-Loève Expansion, the definition of the ply orientations in Eq. (31) may be rewritten as

$$\theta_i(\omega, \mathbf{x}) = \theta_{i0} + \sigma \sum_{j=1}^m \sqrt{\lambda_j} \varphi_j(\mathbf{x}) \zeta_{ij}(\omega) = \theta_{i0} + \sigma \sum_{j=1}^m \eta_j(\mathbf{x}) \zeta_{ij}(\omega) \quad (55)$$

where λ_j , $\zeta_j(\omega)$, and $\varphi_j(\mathbf{x})$ are as defined in Eq. (16), and $\eta_j(\mathbf{x})$ is introduced to group together the non-random parts of each KLE term for the sake of conciseness. The lamination parameters are approximated as a sum of basis polynomials, $\Psi_q(\omega)$ in $m \times n$ random variables, which are expressed as

$$\Psi_q(\omega) = \prod_{i=1}^n \prod_{j=1}^m H_{\alpha_{ijq}}(\zeta_{ij}(\omega)) \quad (56)$$

where multi-index α_{ijq} is modified from Eq. (34) to dictate the order of the polynomial corresponding to the j^{th} KLE term in the i^{th} ply, in the q^{th} basis function.

Expansion coefficients for ξ_1^A may once again be derived by setting the residuals as orthogonal to the basis functions in line with the numerator of Eq. (28), which may be expressed as

$$\mathbb{E}[\xi_1^A(\omega, \mathbf{x}) \Psi_q(\omega)] = \frac{1}{2} \sum_{i=1}^n (u_{i+1} - u_i) \mathbb{E} \left[\cos(2\theta_i(\omega, \mathbf{x})) \prod_{j=1}^n H_{\alpha_{ijq}}(\zeta_{ij}(\omega)) \right] \prod_{\substack{k=1 \\ k \neq i}}^n \prod_{j=1}^m \mathbb{E}[H_{\alpha_{kjq}}(\zeta_{kj}(\omega))] \quad (57)$$

As in the random variable case study, this expectation is zero in all cases in which α_{ijq} is greater than zero for multiple values of i , and the coefficients which model the interaction between different plies are all zero. In all other cases the

expectation is given by

$$\mathbb{E}[\xi_1^A(\omega, \mathbf{x})\Psi_q(\omega)] = \begin{cases} \frac{1}{2} \sum_{i=1}^n (u_{i+1} - u_i) \mathbb{E}[\cos(2\theta_i(\omega, \mathbf{x}))] & \text{if } \alpha_{ijq} = 0 \forall i, j \\ \frac{1}{2} (u_{i+1} - u_i) \mathbb{E}[\cos(2\theta_i(\omega, \mathbf{x})) \prod_{j=1}^m H_{\alpha_{ijq}}(\zeta_{ij}(\omega))] & \text{for } i \text{ s.t. } \sum_{j=1}^m \alpha_{ijq} > 0 \end{cases} \quad (58)$$

It should be noted that this expression differs from that in Eq. (36), in that there are interactions between the different KLE terms within each ply. Uncertainty in the different plies is represented using an identical set of polynomials, and as such, the i may be dropped in the subscript of multi-index α .

Starting with the second case of Eq. (58), the expectation may be expanded by exploiting the independence of the random variables, and using the compound angle formulae to obtain

$$\begin{aligned} \mathbb{E}[\xi_1^A(\omega, \mathbf{x})\Psi_q(\omega)] &= \frac{1}{2} (u_{i+1} - u_i) \\ &\times \left(\mathbb{E} \left[\cos(2\sigma\eta_1(\mathbf{x})\zeta_{i1}(\omega)) H_{\alpha_{1q}}(\zeta_{i1}(\omega)) \right] \mathbb{E} \left[\cos \left(2\theta_{i0} + 2\sigma \sum_{j=2}^m \eta_j(\mathbf{x})\zeta_{ij}(\omega) \right) \prod_{j=2}^m H_{\alpha_{jq}}(\zeta_{ij}(\omega)) \right] \right. \\ &\left. - \mathbb{E} \left[\sin(2\sigma\eta_1(\mathbf{x})\zeta_{i1}(\omega)) H_{\alpha_{1q}}(\zeta_{i1}(\omega)) \right] \mathbb{E} \left[\sin \left(2\theta_{i0} + 2\sigma \sum_{j=2}^m \eta_j(\mathbf{x})\zeta_{ij}(\omega) \right) \prod_{j=2}^m H_{\alpha_{jq}}(\zeta_{ij}(\omega)) \right] \right) \end{aligned} \quad (59)$$

In Eq. (59), the first KLE term is separated into its own univariate expectation. Noting that $\zeta_{1j}(\omega)$ is a standard Gaussian variable, the expectation of the $\sin(2\sigma\eta_1(\mathbf{x})\zeta_{i1}(\omega))$ term is zero due to symmetry for even order polynomials, whereas the $\cos(2\sigma\eta_1(\mathbf{x})\zeta_{i1}(\omega))$ term is zero for odd order polynomials. As such, it is always possible to discard one of the terms resulting from the compound angle formulae. This process may be repeated to simplify the resulting expression as the product of the expectation of different univariate Hermite polynomials governed by $H_{\alpha_{jq}}$, factored by the corresponding sin or cos term. These expectations are given by

$$\mathbb{E}[\sin(2\sigma\eta_j(\mathbf{x})\zeta_{ij}(\omega)) H_{\alpha_{jq}}(\zeta_{ij}(\omega))] = \begin{cases} 2\sigma(-4\sigma^2)^{\frac{\alpha_{jq}-1}{2}} \eta_j(\mathbf{x})^{\alpha_{jq}} e^{-2\sigma^2\eta_j(\mathbf{x})^2} & \text{if } \alpha_{jq} \text{ is odd} \\ 0 & \text{if } \alpha_{jq} \text{ is even} \end{cases} \quad (60)$$

and

$$\mathbb{E}[\cos(2\sigma\eta_j(\mathbf{x})\zeta_{ij}(\omega)) H_{\alpha_{jq}}(\zeta_{ij}(\omega))] = \begin{cases} 0 & \text{if } \alpha_{jq} \text{ is odd} \\ (-4\sigma^2)^{\frac{\alpha_{jq}}{2}} \eta_j(\mathbf{x})^{\alpha_{jq}} e^{-2\sigma^2\eta_j(\mathbf{x})^2} & \text{if } \alpha_{jq} \text{ is even} \end{cases} \quad (61)$$

The first case of Eq. (58), corresponding to the first expansion coefficient $\hat{\alpha}_0$, is a specific example of Eq. (59) with

$\alpha_{j0} = 0 \forall j$, summed over every ply of the laminate. This coefficient is therefore given by

$$\mathbb{E}[\xi_1^A(\omega, \mathbf{x})\Psi_0(\omega)] = \frac{1}{2} \sum_{i=1}^n (u_{i+1} - u_i) \cos(2\theta_{i0}) \prod_{j=1}^m \mathbb{E}[\cos(2\sigma\eta_j(\mathbf{x})\zeta_{ij}(\omega))] = \xi_{10}^A e^{-2\sigma^2 \sum_{j=1}^m \eta_j(\mathbf{x})^2} \quad (62)$$

which is simply the expression given in Eq. (37) for the random variable case study, with additional factors due to the contribution of the KLE eigenvalues and eigenfunctions to the variance of the approximated random field.

To complete the expansion, expressions are required for the normalising coefficients given by the denominator of Eq. (28). Noting that it is necessary to account for the interactions between the different KLE terms, and using the result from Eq. (39), the normalising coefficients can be shown to be given by

$$\mathbb{E} \left[\prod_{j=1}^m H_{\alpha_{jq}}(\zeta_{ij}(\omega))^2 \right] = \prod_{j=1}^m \alpha_{jq}! \quad (63)$$

The Polynomial Chaos Expansion for $\xi_1^A(\omega, \mathbf{x})$ can therefore be expressed as

$$\begin{aligned} \xi_1^A(\omega, \mathbf{x}) &\approx e^{-2\sigma^2 \sum_{j=1}^m \eta_j(\mathbf{x})^2} \\ &\times \left(\xi_{10}^A - \frac{1}{2} \sum_{\substack{\alpha_q \in \alpha \\ |\alpha_q| \text{ is odd}}} 2\sigma(-4\sigma^2)^{\frac{|\alpha_q|-1}{2}} \left(\prod_{j=1}^m \frac{\eta_j(\mathbf{x})^{\alpha_{jq}}}{\alpha_{jq}!} \right) \sum_{i=1}^n (u_{i+1} - u_i) \sin(2\theta_{i0}) \prod_{j=1}^m H_{\alpha_{jq}}(\zeta_{ij}(\omega)) \right. \\ &\left. + \frac{1}{2} \sum_{\substack{\alpha_q \in \alpha \\ |\alpha_q| \text{ is even}}} (-4\sigma^2)^{\frac{|\alpha_q|}{2}} \left(\prod_{j=1}^m \frac{\eta_j(\mathbf{x})^{\alpha_{jq}}}{\alpha_{jq}!} \right) \sum_{i=1}^n (u_{i+1} - u_i) \cos(2\theta_{i0}) \prod_{j=1}^m H_{\alpha_{jq}}(\zeta_{ij}(\omega)) \right) \end{aligned} \quad (64)$$

where $|\alpha_k| = \sum_{j=1}^m \alpha_{jk}$. Following the same process, the Polynomial Chaos Expansion for general lamination parameter $\xi_k^l(\omega)$ may be derived as

$$\begin{aligned} \xi_k^l(\omega, \mathbf{x}) &\approx e^{-\frac{1}{2}a^2\sigma^2 \sum_{j=1}^m \eta_j(\mathbf{x})^2} \\ &\times \left(\xi_{k0}^l + \frac{1}{2} \sum_{\substack{\alpha_q \in \alpha \\ |\alpha_q| \text{ is odd}}} a\sigma(-a^2\sigma^2)^{\frac{|\alpha_q|-1}{2}} \left(\prod_{j=1}^m \frac{\eta_j(\mathbf{x})^{\alpha_{jq}}}{\alpha_{jq}!} \right) \sum_{i=1}^n (u_{i+1}^b - u_i^b)g(a\theta_{i0}) \prod_{j=1}^m H_{\alpha_{jq}}(\zeta_{ij}(\omega)) \right. \\ &\left. + \frac{1}{2} \sum_{\substack{\alpha_q \in \alpha \\ |\alpha_q| \text{ is even}}} (-a^2\sigma^2)^{\frac{|\alpha_q|}{2}} \left(\prod_{j=1}^m \frac{\eta_j(\mathbf{x})^{\alpha_{jq}}}{\alpha_{jq}!} \right) \sum_{i=1}^n (u_{i+1}^b - u_i^b)f(a\theta_{i0}) \prod_{j=1}^m H_{\alpha_{jq}}(\zeta_{ij}(\omega)) \right) \end{aligned} \quad (65)$$

where a, b, f, g, k , and l are as defined in relations to Eq. (41). It can be seen that Eqs. (64-65) take a similar form to Eqs. (40-41), with the addition of extra terms to capture the effects of the KLE eigenvalues and eigenfunctions upon the ply orientation variance, and the interaction between the different KLE terms within each ply.

Realisations of the lamination parameters may be simulated using the basis functions, $\Psi_q(\omega)$, however, the number of basis functions is by definition larger than the number of plies. It can be seen from Eq. (65), that the spatial

dependency is outside of the sum over the laminate thickness. It is possible to preserve the separation of the spatial and random terms while simulating the lamination parameters at the laminate level, using an expansion of the form

$$\xi_k^l(\omega, \mathbf{x}) \approx e^{-\frac{1}{2}a^2\sigma^2\sum_{j=1}^m\eta_j(\mathbf{x})^2}\left(\xi_{k0}^l + \sum_{q=1}^{N_{RV}}h_q(\mathbf{x})\Upsilon_q(\omega)\right) \quad (66)$$

where

$$\Upsilon_q(\omega) = \begin{cases} \sum_{i=1}^n(u_{i+1}^b - u_i^b)g(a\theta_{i0})\prod_{j=1}^m H_{\alpha_{jq}}(\zeta_{ij}(\omega)) & \text{if } |\alpha_q| \text{ is odd} \\ \sum_{i=1}^n(u_{i+1}^b - u_i^b)f(a\theta_{i0})\prod_{j=1}^m H_{\alpha_{jq}}(\zeta_{ij}(\omega)) & \text{if } |\alpha_q| \text{ is even} \end{cases} \quad (67)$$

where N_{RV} is the number of random variables, and $h_q(\mathbf{x})$ is used to group together all parts of the expansion coefficients in Eq. (65) which lie outside of the through thickness sum.

B. Number of Random Variables

The overall aim of the proposed approach is to reduce the number of random variables compared with that required to directly model uncertainty in the ply orientations. For random variable ply orientations, the lamination parameters may be simulated directly using commonly used techniques such as Monte Carlo Simulation.³² In the most general case, the maximum number of random variables is therefore twelve. As such, a laminate must have at least twelve plies for there to be an advantage in general.

For random fields, it is not possible to directly simulate the lamination parameters, which are highly non-Gaussian. The proposed combination of Karhunen-Loève Expansion and Polynomial Chaos Expansion enables the lamination parameters to be simulated using the $\Upsilon_q(\omega)$ terms given by Eq. (67), however, the number of random variables depends upon the number of KLE terms used to model the ply orientation uncertainty, and the order of the polynomial Chaos. The number of random variables required to simulate random fields in all twelve lamination parameters is given by

$$N_{RV} = 12\left(\frac{(m+p)!}{m!p!} - 1\right) \quad (68)$$

Using Eq. (68), the required number of random variables is shown in Table 2 for various orders of polynomial chaos and numbers of KLE terms. If the uncertainty is modelled directly using the ply orientations, the number of random variables is simply the number of plies multiplied by the number of KLE terms. As in the random variable case, a laminate must have a minimum number of plies before there is a benefit to using lamination parameters. This minimum number of plies, n_{\min} , is also shown in Table 2, given by N_{RV}/N_{KLE} .

Supposing five KLE terms were used to model uncertainty in each ply in conjunction with a 2nd order Polynomial Chaos Expansion. From Table 2 it can be seen that the lamination parameters may be simulated using 240 random variables. This is equivalent to modelling uncertainty in 48 ply orientations, using 5×48 KLE terms. As such, the

KLE Terms	Order							
	2		3		4		5	
	N_{RV}	n_{min}	N_{RV}	n_{min}	N_{RV}	n_{min}	N_{RV}	n_{min}
2	60	30	108	54	168	84	240	120
5	240	48	660	132	1,500	300	3,012	603
10	780	78	3,420	342	12,000	1,200	36,024	3,603
25	4,200	168	39,300	1,572	285,000	11,400	1,710,060	68,403

Table 2: Number of variables required to model field, and minimum number of plies for which a benefit is achieved

number of random variables may be reduced for any laminate with more than 48 plies. For example, the number of random variables could be reduced by 10 for a laminate with 50 plies.

The number of variables can be seen to scale highly unfavourably with the number of terms used in the KLE. As such, it is suggested that the proposed approach is unlikely to achieve any benefits for greater than a 2nd order expansion. Additionally, the approach would achieve greatest benefits modelling uncertainty in a large number of ply orientations, as random fields with a high correlation length such that relatively few KLE terms are required. For a larger number of KLE terms, it is possible that a spatial discretisation would be more efficient, as it may be possible to achieve a sufficiently fine mesh in with fewer random variables.

C. Comparison with Monte Carlo Simulation

In this section, the expression derived in the previous sections are compared against Monte Carlo Simulation of the out-of-plane lamination parameters of a $[0_2, 90_2]_S$ laminate. A ply orientation standard deviation of 5° is used in order to highlight limitations in modelling a relatively large magnitude of uncertainty, and a correlation length of $L/2$ is used along with 20 KLE terms, which corresponds to the scenario in Figure 2b). Example realisations of one-dimensional random fields obtained using a 2nd order Polynomial Chaos Expansion are compared with Monte Carlo results based upon the same Karhunen-Loève Expansion in Figure 9. Assuming the random field is stationary, estimates of the marginal distributions are shown in Figure 10, based upon an ensemble average taken across 1000 points in the spatial domain, and estimates of the covariance function based upon 10,000 field realisations are shown in Figure 11. In these plots the Monte Carlo results are obtained using a spatial discretisation of the random field, rather than KLE.

From Figure 9 it can be seen that the 2nd order expansion achieves a good match with Monte Carlo results, with some small discrepancies in the realisations of ξ_2^D and ξ_4^D , which may be attributed to the fact that in these lamination parameters the ply orientation uncertainty is multiplied by a factor of 4 rather than 2. The marginal distributions in Figure 10 show that the distributions of ξ_{3-4}^D are approximately Gaussian, which is reflected by the fact that the example realisations fall either side of the deterministic values. The marginals of ξ_{1-2}^D are highly skewed, and as such the realisations tend to lie below the deterministic value for these lamination parameters. In line with these observations, a 1st order expansion is sufficient to accurately model ξ_{3-4}^D , whereas a 2nd order expansion is necessary

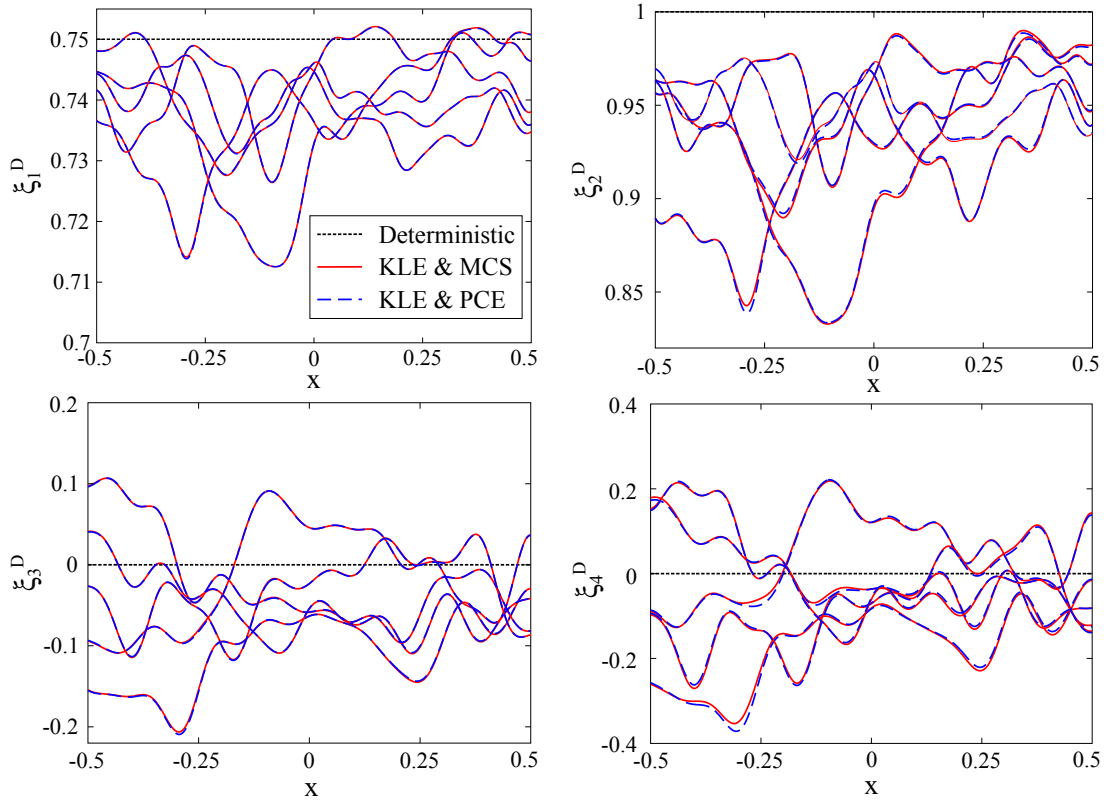


Figure 9: Random field realisations for the out-of-plane lamination parameters of a $[0_2, 90_2]_S$ laminate

to model the non-Gaussian behaviour in ξ_{1-2}^D . In this case, a minimum 2nd order expansion is required, as the odd coefficients are zero due to their dependency upon $\sin(2\theta_{i0})$ and $\sin(4\theta_{i0})$ in Eq. (65). The same observation may be made about the even coefficients of ξ_{3-4}^D . For this reason, the required number of random variables may be fewer than that shown in Eq. (68) if restrictions are placed upon the layup.

As in the example realisations, some error may be noted in the marginal PDFs for the 2nd order expansion of ξ_2^D and ξ_4^D . Although a slight reduction in error may be achieved by using higher order expansions, it can be noted from Table 2 that the number of random variables increases substantially with the order of the polynomials. It is therefore suggested that a 2nd order expansion is used as a reasonable compromise between accuracy and efficiency.

From Figure 11, it can be seen that very little improvement in the covariance function occurs with increasing polynomial order, despite the evident errors in the approximation. These errors may be attributed to the truncation of the Karhunen-Loève Expansion, and as such, larger errors may be noted for small differences in x , which require additional KLE terms. The KLE also results in a smooth approximation of the covariance function at $|x - x'| = 0$, where the actual covariance function is non-smooth.

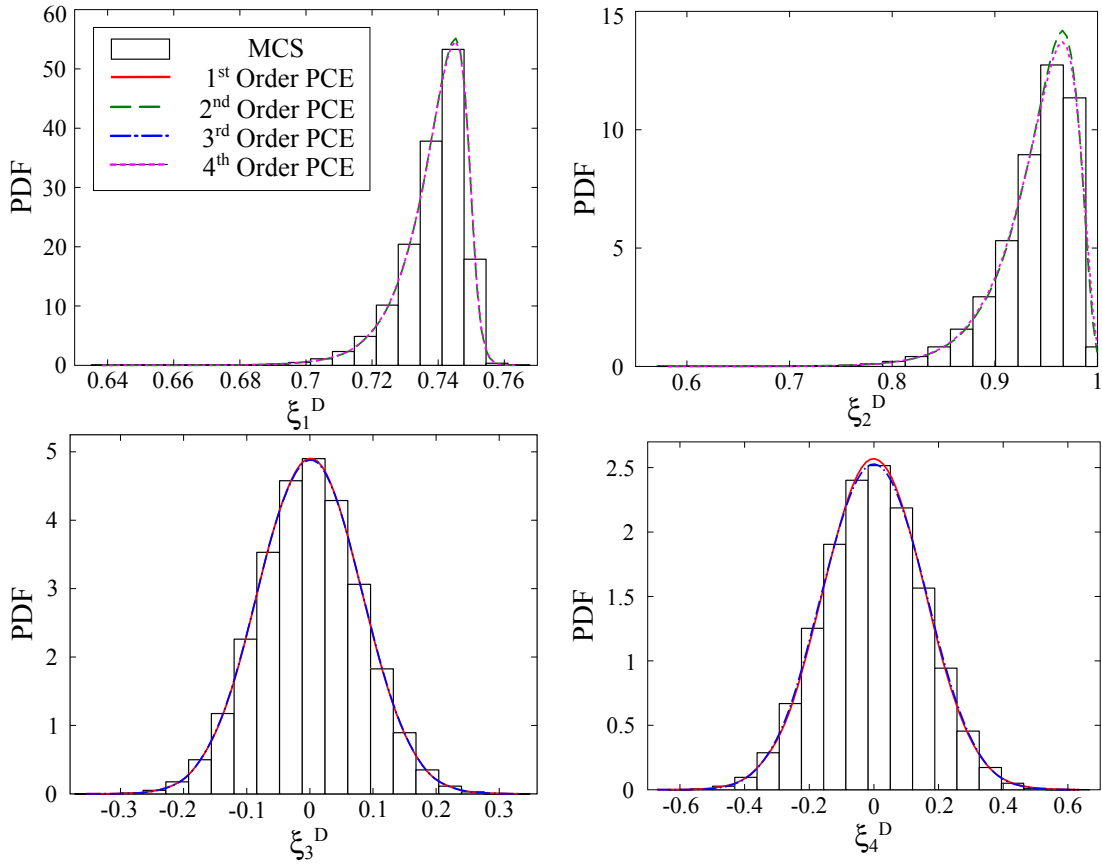


Figure 10: Marginal PDFs for the out-of-plane lamination parameters of a $[0_2, 90_2]_S$ laminate

VI. Conclusions

A method for modelling spatially varying uncertainty in composite ply orientations has been presented. Karhunen-Loève Expansion is used to decompose the random fields, and an intrusive Polynomial Chaos Expansion is derived for the lamination parameters. The aim of the proposed approach was to represent the uncertainty using a reduced number of random variables, while ensuring the separation of the random and spatial dependency of the random field at a laminate level. Closed-form expressions for the expansion have been derived in two case studies; an initial example in which the uncertainty defined using random variables, and a second in which the uncertainty is defined using random fields. The proposed approach is a ‘bottom-up’ method for defining laminate properties based upon uncertain ply-level properties. Such an approach enables laminate-level properties to be modelled, while preserving the separation of random and spatial dependency achieved using a KLE defined at the laminate level.

The number of random variables required by the Polynomial Chaos Expansion was by definition found to be greater than or equal to the number of plies. In the random field example, it was noted that the spatially dependent terms may be separated from the through-thickness sum, and the field simulated more efficiently using the summed random variables. The number of random variables was found to scale nonlinearly with the number of KLE terms and polynomial order,

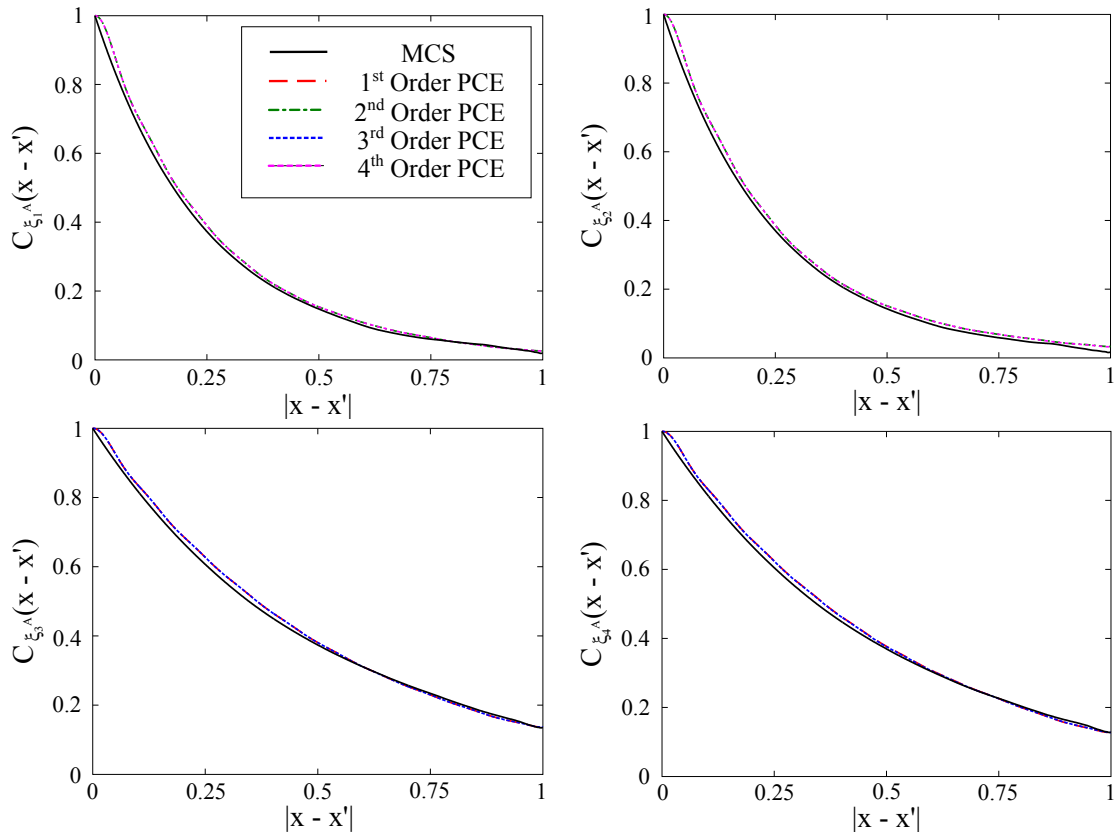


Figure 11: Correlation functions for the out-of-plane lamination parameters of a $[0_2, 90_2]_S$ laminate

and as such, there is a minimum number of plies for which the proposed approach is beneficial over directly modelling the ply orientation uncertainty. The approach is therefore only beneficial in low order expansions, for laminates with a large number of plies.

It was found that the error in the expansion reduced exponentially with increasing polynomial order, with the polynomial chaos approximation converging to exact closed-form expressions for the covariance for infinite polynomial order. A minimum 2nd order expansion was typically sufficient to achieve a good agreement with benchmark Monte Carlo results, and given the unfavourable scaling with polynomial order, this is considered a reasonable compromise between accuracy and efficiency.

References

- ¹C C Chamis. Probabilistic Simulation of Multi-scale Composite Behavior. *Theoretical and Applied Fracture Mechanics*, 41(1-3):51–61, 2004.
- ²K Potter, B Khan, M Wisnom, T Bell, and J Stevens. Variability, Fibre Waviness and Misalignment in the Determination of the Properties of Composite Materials and Structures. *Composites Part A: Applied Science and Manufacturing*, 39(9):1343–1354, 2008.
- ³Srinivas Sriramula and Marios K. Chryssanthopoulos. Quantification of Uncertainty Modelling in Stochastic Analysis of FRP Composites. *Composites Part A: Applied Science and Manufacturing*, 40(11):1673–1684, 2009.

- ⁴Chris L. Pettit. Uncertainty Quantification in Aeroelasticity: Recent Results and Research Challenges. *Journal of Aircraft*, 41(5):1217–1229, 2004.
- ⁵Robert E Melchers. *Structural reliability: Analysis and Prediction*. John Wiley & Sons Ltd, Chichester, West Sussex, UK, 2nd edition, 1999.
- ⁶Roger G Ghanem and Pol D Spanos. *Stochastic Finite Elements: A Spectral Approach*. Springer-Verlag, New York, 1991.
- ⁷D Xiu and G Karniadakis. The Wiener-Askey Polynomial Chaos for Stochastic Differential Equations. *SIAM Journal on Scientific Computing*, 24(2):619–644, 2002.
- ⁸Bruno Sudret and Armen Der-Kiureghian. Stochastic Finite Element Methods and Reliability. Technical report, Department of Civil & Environmental Engineering, University of California, Berkeley, 2000.
- ⁹S Murugan, R Ganguli, and D Harursampath. Aeroelastic Response of Composite Helicopter Rotor with Random Material Properties. *Journal of Aircraft*, 45(1):306–322, 2008.
- ¹⁰D G Liaw and Henry T Y Yang. Reliability of Initially Compressed Uncertain Laminated Plates in Supersonic Flow. *AIAA Journal*, 29(6):952–960, 1991.
- ¹¹D H Oh and L Librescu. Free Vibration and Reliability of Composite Cantilevers featuring Uncertain Properties. *Reliability Engineering & System Safety*, 56(3):265–272, 1997.
- ¹²Abdul Manan and Jonathan Cooper. Design of Composite Wings Including Uncertainties: A Probabilistic Approach. *Journal of Aircraft*, 46(2):601–607, 2009.
- ¹³K Umesh and Ranjan Ganguli. Material Uncertainty Effect on Vibration Control of Smart Composite Plate Using Polynomial Chaos Expansion. *Mechanics of Advanced Materials and Structures*, 20(7):580–591, 2012.
- ¹⁴Sudip Dey, Tanmoy Mukhopadhyay, and Sondipon Adhikari. Stochastic Free Vibration Analyses of Composite Shallow Doubly Curved Shells - A Kriging Model Approach. *Composites Part B: Engineering*, 70:99–112, 2015.
- ¹⁵Sudip Dey, Tanmoy Mukhopadhyay, and Sondipon Adhikari. Stochastic Free Vibration Analysis of Angle-ply Composite Plates - A RS-HDMR Approach. *Composite Structures*, 122:526–536, 2015.
- ¹⁶S Dey, T Mukhopadhyay, H Haddad Khodaparast, and S Adhikari. Fuzzy Uncertainty Propagation in Composites using Gram-Šchmidt Polynomial Chaos Expansion. *Applied Mathematical Modelling*, 40(7):4412–4428, 2016.
- ¹⁷Sudip Dey, Tanmoy Mukhopadhyay, S Adhikari, Axel Spickenheuer, and Uwe Gohs. Uncertainty quantification in Natural Frequency of Composite Plates: an Artificial Neural Network Based Approach. *Advanced Composite Letters*, 25(2):43–48, 2016.
- ¹⁸S P Engelstad and J N Reddy. Probabilistic Nonlinear Finite Element Analysis of Composite Structures. *AIAA Journal*, 31(2):362–369, 1993.
- ¹⁹P Venini and C Mariani. Free Vibrations of Uncertain Composite Plates via Stochastic Rayleigh-Ritz Approach. *Computers & Structures*, 64(1):407–423, 1997.
- ²⁰M F Ngah and A Young. Application of the Spectral Stochastic Finite Element Method for Performance Prediction of Composite Structures. *Composite Structures*, 78(3):447–456, 2007.
- ²¹Senthil Murugan, R. Chowdhury, S. Adhikari, and M. I. Friswell. Helicopter Aeroelastic Analysis with Spatially Uncertain Rotor Blade Properties. *Aerospace Science and Technology*, 16(1):29–39, 2012.
- ²²K Sepahvand. Spectral Stochastic Finite Element Vibration Analysis of Fiber-Reinforced Composites with Random Fiber Orientation. *Composite Structures*, 145:119–128, 2016.
- ²³P Sasikumar, R Suresh, and Sayan Gupta. Analysis of CFRP Laminated Plates with Spatially Varying Non-Gaussian Inhomogeneities using SFEM. *Composite Structures*, 112:308–326, 2014.
- ²⁴P Sasikumar, A Venketeswaran, R Suresh, and Sayan Gupta. A Data Driven Polynomial Chaos Based Approach for Stochastic Analysis of CFRP Laminated Composite Plates. *Composite Structures*, 125:212–227, 2015.

- ²⁵Mitsunori Miki. Material Design of Composite Laminates with Required In-Plane Elastic Properties. *Proc Progress in Science and Engineering of Composites, ICCM IV, Tokyo*, 1982.
- ²⁶Mitsunori Miki and Yoshihiko Sugiyamat. Optimum Design of Laminated Composite Plates Using Lamination Parameters. *AIAA Journal*, 31(5):921–922, 1993.
- ²⁷Stephen W Tsai, John C Halpin, and Nicolas J Pagano. Composite Materials Workshop. 1968.
- ²⁸Hisao Fukunaga and Hideki Sekine. Stiffness Design Method of Symmetric Laminates using Lamination Parameters. *AIAA Journal*, 30(11):2791–2793, 1992.
- ²⁹J L Grenestedt and P Gudmundson. Layup Optimization of Composite Material Structures. In *Proceedings of the IUTAM Symposium on Optimal design with advanced materials*, pages 311–336, Amsterdam, The Netherlands, 1993. Elsevier Science.
- ³⁰J. Enrique Herencia, Paul M. Weaver, and Michael I. Friswell. Optimization of Anisotropic Composite Panels with T-shaped Stiffeners Including Transverse Shear Effects and Out-of-Plane Loading. *Structural and Multidisciplinary Optimization*, 37(2):165–184, 2008.
- ³¹M W Bloomfield, C G Diaconu, and P M Weaver. On Feasible Regions of Lamination Parameters for Lay-up Optimization of Laminated Composites. *Proceedings of the Royal Society A: Mathematical, Physical and Engineering Sciences*, 465:1123–1143, 2009.
- ³²Carl Scarth, Jonathan E. Cooper, Paul M. Weaver, and Gustavo H C Silva. Uncertainty Quantification of Aeroelastic Stability of Composite Plate Wings using Lamination Parameters. *Composite Structures*, 116(1):84–93, 2014.
- ³³S W Tsai and H T Hahn. *Introduction to Composite Materials*. CT: Technomic Publishing Co., Inc, Lancaster, 1980.
- ³⁴Mircea Grigoriu. Simulation of Stationary Non-Gaussian Translation Processes. *Journal of Engineering Mechanics*, 124(2):121–126, 1998.
- ³⁵Paolo Bocchini and George Deodatis. Critical Review and Latest Developments of a Class of Simulation Algorithms for Strongly Non-Gaussian Random Fields. *Probabilistic Engineering Mechanics*, 23(4):393–407, 2008.